

Efficient Federated Learning with Heterogeneous Data and Adaptive Dropout

JI LIU^{*†}, Baidu Research and Hithink RoyalFlush Information Network Co., Ltd., China

BEICHEN MA[†], Baidu Research, China and Cornell University, United States

QIAOLIN YU, Cornell University, United States

RUOMING JIN, Kent State University, United States

JINGBO ZHOU, BIL, Baidu Research, China

YANG ZHOU, Department of Computer Science and Software Engineering, Auburn University, United States

HUAIYU DAI, Department of Electrical and Computer Engineering, North Carolina State University, United States

HAIXUN WANG, Instacart, United States

DEJING DOU, BEDI Cloud and School of Computer Science, Fudan University, China

PATRICK VALDURIEZ, Inria, University of Montpellier, CNRS, LIRMM, France and LNCC, Brazil

Federated Learning (FL) is a promising distributed machine learning approach that enables collaborative training of a global model using multiple edge devices. The data distributed among the edge devices is highly heterogeneous. Thus, FL faces the challenge of data distribution and heterogeneity, where non-Independent and Identically Distributed (non-IID) data across edge devices may yield in significant accuracy drop. Furthermore, the limited computation and communication capabilities of edge devices increase the likelihood of stragglers, thus leading to slow model convergence. In this paper, we propose the FedDHAD FL framework, which comes with two novel methods: Dynamic Heterogeneous model aggregation (FedDH) and Adaptive Dropout (FedAD). FedDH dynamically adjusts the weights of each local model within the model aggregation process based on the non-IID degree of heterogeneous data to deal with the statistical data heterogeneity. FedAD performs neuron-adaptive operations in response to heterogeneous devices to improve accuracy while achieving superb efficiency. The combination of these two methods makes FedDHAD significantly outperform state-of-the-art solutions in terms of accuracy (up to 6.7% higher), efficiency (up to 2.02 times faster), and computation cost (up to 15.0% smaller).

Additional Key Words and Phrases: Federated learning, heterogeneous data, adaptive dropout, distributed machine learning, device heterogeneity

1 Introduction

Ever growing, high numbers of edge devices (devices for short) generate huge amounts of distributed data that can be very useful for machine learning. To avoid the common problems of a centralized approach (high data transfer cost, long training time, ...), Federated Learning (FL) [1–3] collaboratively trains a global model using multiple edge devices. While the data generally contain sensitive information about end-users, e.g., facial images, location-based services, and account information

^{*}Corresponding author: jiliuwork@gmail.com

[†]Both authors contributed equally to this research.

Authors' Contact Information: Ji Liu, Baidu Research and Hithink RoyalFlush Information Network Co., Ltd., Hangzhou, China; Beichen Ma, Baidu Research, China and Cornell University, New York, United States; Qiaolin Yu, Cornell University, New York, United States; Ruoming Jin, Kent State University, Kent, Ohio, United States; Jingbo Zhou, BIL, Baidu Research, Beijing, China; Yang Zhou, Department of Computer Science and Software Engineering, Auburn University, Auburn, United States; Huaiyu Dai, Department of Electrical and Computer Engineering, North Carolina State University, North Carolina, United States; Haixun Wang, Instacart, San Francisco, California, United States; Dejing Dou, BEDI Cloud and School of Computer Science, Fudan University, Beijing, China; Patrick Valduriez, Inria, University of Montpellier, CNRS, LIRMM, France and LNCC, Petropolis, Rio de Janeiro, Brazil.

[4], multiple legal restrictions [5, 6] protect the privacy and security of distributed data, so that data aggregation from distributed devices is almost impossible. Within a typical FL architecture [7], a powerful parameter server module (server for short) [8, 9] coordinates the training process of multiple devices and aggregates the trained models instead of the raw data from the devices, thus providing security and privacy.

As multiple devices may belong to various end-users, the data that is distributed among the edge devices is highly heterogeneous [10–12] in terms of distribution, *i.e.*, non-Independent and Identically Distributed (non-IID) [7]. While data format or semantics are generally homogeneous, the statistical data distribution among devices is highly heterogeneous [13]. For instance, the proportion of the samples corresponding to Class A on a device can be very different from that of other devices. While FL was proposed to train a global model using non-IID data on mobile devices [7, 14], the traditional FL models may incur inferior accuracy [15] brought by such statistical data heterogeneity. The training process of FL generally corresponds to multiple rounds, each with three steps. In Step 1, the server sends the global model to selected devices. In Step 2, the selected devices update the global model with local data and upload the updated model to the server. In Step 3, the server performs the model aggregation with the uploaded models. Conventional model aggregation methods, *e.g.*, FedAvg [7], ignore the property of non-IID data while aggregating the local models, which would lower accuracy.

Recent techniques have improved the performance of FL on non-IID data using additional proximal terms (Step 2) in the local update, *e.g.*, FedProx [15], or based on gradient normalization and averaged steps in the model aggregation (Step 3), *e.g.*, FedNova [10]. However, the trained model still suffers from data heterogeneity. The performance of the trained model may be unacceptably poor, and the training process may even become unstable in practice. We quantify the heterogeneity between the distribution of the dataset on a device and that of all the datasets on all available devices by non-IID degree using Formula 12 (see details in Section 5.1.3). Although the Jensen–Shannon (JS) divergence [16] or Kullback–Leibler (KL) divergence [17] can be exploited, there is still a difference between JS and KL divergences and the non-IID degree.

To alleviate the statistical data heterogeneity issue, a promising solution is to adapt for each model the weight tuning to the non-IID degree. The global model optimization with weight tuning can be formulated as a bi-level optimization problem [18], where the global model optimization and the weight adjustment belong to the optimization of two levels. However, there are two major difficulties in finding the optimal weights of each model, which is critical for the training process of FL. First, the training process dynamically varies and the optimal weights may vary in various epochs. Second, it is difficult to accurately calculate the non-IID degrees, which are critical for the optimal weights.

While the server is generally powerful, some devices typically have modest computation and communication capacities [7]. For instance, in a real phone keyboard application [19], 6-10% devices may take an unaccepted long time to return the updated models. Such device heterogeneity leads to slow model convergence due to low efficiency of the local training process and unbalanced workload. High-dimensional model parameters (*e.g.*, deep neural networks) in the FL paradigm give rise to extremely high computation and communication overhead. Within a standard FL environment, the bandwidth between the devices and server is generally of low quality. Furthermore, models become bigger and bigger, especially for Large Language Models (LLM), to achieve superb performance, which incurs significant computation and communication costs. Thus, it takes much time to send the global model from the server to the devices or to upload the updated models from each device to the server. In addition, heterogeneous hardware resources across devices increase the likelihood of stragglers, *i.e.*, the slowest participating devices, which incur an unbalanced workload.

Dropout techniques [20] randomly remove neurons during training to reduce overfitting and to achieve superior performance. They have been exploited in FL for reducing the size of the global

model and thus communication and computation cost [21]. However, the straightforward application of dropout to FL may incur significant accuracy degradation of the global model [22] with improper dropout rates [23]. In order to fully exploit the heterogeneous devices, adaptive pruning rates should be utilized. Furthermore, model aggregation with dropout becomes even more challenging than without dropout as it is hard to verify the importance of the updated models with some neurons removed. Thus, it is critical to dynamically adjust the weights with the adaptive pruning operation.

Statistical data heterogeneity and device heterogeneity are often regarded as orthogonal problems, which are addressed separately. However, solving either problem leads to inaccurate and inefficient analytical results. Some methods can be exploited to address the non-IID data issue, *e.g.*, regularization-based method [15, 24], gradient normalization [10], contrastive learning [25], client drift adjustment [26], and personalization [27]. Some other methods have been addressed the device heterogeneity problem, *e.g.*, asynchronous staleness aggregation [28–32]. However, some of them can be combined with our approach to achieve superior performance.

In this paper, we propose the FedDHAD framework to simultaneously address the data heterogeneity and the heterogeneous limited capacity problem. We propose exploiting the non-IID degrees of devices to dynamically adjust the weights of each local model within the model aggregation process, *i.e.*, FedDH, in order to alleviate the impact of the heterogeneous data. Then, we introduce a neuron-adaptive model dropout method, *i.e.*, FedAD, to perform the dropout operation adapted to each device while achieving load balancing so as to reduce the communication and computation cost and to achieve a good balance between efficiency and effectiveness. While FedAD can compensate the slight overhead brought by FedDH, we integrate these two methods into FedDHAD, thus accelerating the training process and improving accuracy. We conduct extensive experiments to compare FedDHAD with representative approaches with two typical models over two real-world datasets. Experimental results demonstrate the major advantages of FedDHAD in terms of accuracy, efficiency, and computation cost. The major contributions are summarized as follows:

- We propose a Dynamic Heterogeneous model aggregation algorithm for non-IID data, *i.e.*, FedDH. FedDH takes advantage of the non-IID degree of devices and dynamically adjusts the weights of local models within the model aggregation process.
- We propose an Adaptive Dropout method, *i.e.*, FedAD. FedAD carries out dropout operations adapted to each neuron and diverse idiosyncrasies, *i.e.*, heterogeneous communication and computation capacity, of each device to improve the efficiency of the training process.
- We conduct extensive experiments to compare FedDHAD with representative approaches with two typical models over two real-world datasets. Experimental results demonstrate the superb advantages of FedDHAD in terms of accuracy, efficiency, and computation cost.

The rest of this paper is organized as follows. Section 2 provides some background on FL. Section 3 describes related work. Section 4 introduces the system model of FedDHAD. In Section 5, we describe the FedDHAD framework, including the FedDH and FedAD methods. Section 6, gives our experimental evaluation. Finally, Section 7 concludes.

2 Background on Federal Learning

In this section, we introduce some background concepts on FL. For simplicity, we use the notations summarized in Table 1.

Taxonomy. FL can be classified into cross-silo and cross-device, in terms of participants [1]. The participants of cross-device FL are generally end-users with edge devices, *e.g.*, mobiles. The number of participants is about 100 or bigger. The end-user is the person who generates the raw data for FL. The participants of cross-silo FL generally consist of multiple organizations and the number of participants is generally less than 100. In addition, FL can be further divided according to the kind of

Table 1. Summary of main notations.

Notation	Definition
\mathcal{K}	Set of all devices
t	The number of global round
S_t	The set of selected devices
N	The size of \mathcal{K}
\mathcal{D}_k	Local dataset on Device k
n_k	The size of \mathcal{D}_k
$\mathcal{D}; n$	Global dataset; size of D
d_k	Batch size of the local update of Device k
F	Global loss function
F_k	Local loss function on Device k
w^*	The optimal model
$w_{t,h}^k$	Local model on Device k , Local update h
$\bar{w}_{t,h}$	Global model in the h -th local update
$\eta_{t,h}$	Learning rate in the h -th local update
$\bar{g}_{t,h}$	Global gradients in the h -th local update
τ	Number of local epochs
$\zeta_{t,h}^k$	The sampled dataset at local iteration h on Device k
$ \zeta_{t,h}^k $	The size of $\zeta_{t,h}^k$
$p_{k,t}$	The weights in the model aggregation for Device k

data partitioning, i.e., horizontal, vertical, and hybrid [33]. When the samples from each participant have the same dimensions with the same semantics but correspond to various end-users, the setting is horizontal FL. When the samples of each participant are of different dimensions (various semantics) but correspond to the same end-users, the setting is vertical FL. Otherwise, when the samples of each participants are of different dimensions and correspond to various end-users, the setting is hybrid FL. In this paper, we focus on horizontal cross-device FL. Recent work has explored one-shot semi-supervised FL using pre-trained diffusion models for category-based classification [34]. This approach leverages the power of diffusion models to achieve learning with limited labeled data in a federated setting. In addition, we conduct multiple rounds of training in our system, which deviates from one-shot federated learning [35].

Objectives of FL. In a horizontal cross-device FL environment composed of a powerful server and N devices, we assume that the raw data is distributed at each device and cannot be transferred while there is no raw data on the server for training. We assume that Dataset $D_k = \{x_k, y_k\}^{n_k}$ is located at Device k , consisting of n_k samples. x_k represents the input data sample on Device k , and y_k is the corresponding label. We denote the number of samples on all the devices by n . Then, the objective of the FL training process can be formulated as:

$$\min_w \left[F(w) \triangleq \frac{1}{n} \sum_{k=1}^N n_k F_k(w) \right], \quad (1)$$

where w is the parameters of the global model, $F_k(w)$ is the local loss function of Device k with $f(w, x_k, y_k)$ capturing the error of the model on the sample $\{x_k, y_k\}$, as defined in Formula 2.

$$F_k(w) \triangleq \frac{1}{n_k} \sum_{\{x_k, y_k\} \in \mathcal{D}_k} f(w, x_k, y_k) \quad (2)$$

Table 2. Server computation overhead

	CIFAR10		CIFAR100	
	LeNet	CNN	LeNet	CNN
FedDHAD	0.122	0.156	0.126	0.145
FedDH	0.086	0.042	0.104	0.043

Data heterogeneity. The data is generally highly heterogeneous as the distribution can be both non-identical and non-independent, i.e., non-IID. Let us denote the possibility to get a sample from sampling the local data of Device i by \mathcal{P}_i . Then, the distribution is non-identical when $\mathcal{P}_i \neq \mathcal{P}_j$, where $i \neq j$. The data of each device is non-independent as the end-users may have dependencies on geographic relationships [36]. For instance, the data on the end-users of the same region may have similar patterns. Furthermore, the number of samples on each device can be significantly different.

Challenges. As a *de facto* standard FL approach, FedAvg [7] is a simple yet effective classic approach for FL. With FedAvg, the training process of FL contains three steps in each round as presented in Section 1. In Step 3, FedAvg calculates a simple average model with the updated local models. While the data is highly heterogeneous, the data that severely deviate the global distribution may have important impact on the global model with FedAvg, which may significantly degrade the accuracy of the aggregated model [15]. In addition, the devices are generally of heterogeneous computational and communication capacity. FedAvg transfers the whole model between devices and the server, which incurs significant computational and communication costs and unbalanced workload. Some devices may take an unaccepted time to upload the updated local model, which is inefficient. Thus, device heterogeneity increases the total training time in FL. In this paper, we propose a novel framework, i.e., FedDHAD, to address these two challenges.

3 Related Work

In this section, we introduce the existing FL methods dealing with the model performance issue incurred by data heterogeneity. Then, we present related methods to handle the training efficiency problem.

Conventional methods, e.g., FedAvg [7], can converge with non-IID data [14], while they incur modest accuracy due to inconsistent objectives [10] or client drift [26]. Several methods have been proposed to alleviate the problem. FedProx [15] utilizes regularization in the local objective to tolerate the difference between the local model and the global model. FedCurv [37] calculate global parameter stiffness to control discrepancies. FedDyn [24] further introduces dynamic regularization for each device. FedNova [10] exploits gradient normalization to reduce the influence brought by the heterogeneous learning steps with non-IID data. MOON [25] exploits contrastive learning to adjust the local training based on the similarity of model representations. The primary limitation of these methods is that they concentrate on performance within a single domain under label skew conditions, neglecting the issue of domain shift, resulting in unsatisfactory performance across multiple domains. FedHEAL [38] reduces parameter update conflicts by discarding unimportant parameters and implements fair aggregation to prevent domain bias. However, it requires careful hyperparameter tuning and assumes homogeneous network architectures across all clients, limiting its applicability in heterogeneous settings. Momentum-based methods deal with non-IID data using momentum at the server side or at the device side [39]. Various methods, e.g., partial personalized model aggregation in PartialFed [27], meta-learning-based method [40], and multi-task learning [41], are proposed to realize personalization for non-IID data. ADCOL [42] and FCCL [43] emphasize personalized model training instead of optimizing a single shared global model. However, these approaches necessitate additional components such as discriminators and access to public datasets, imposing significant computational and resource burdens on both participating devices and the central

server. Several other methods [44] align the models within the model aggregation step in order to avoid structural misalignment incurred by the permutation of neural network parameters. In addition, some other works [45] exploit the publicly available data in the server while handling the non-IID, which may incur security or privacy issues. Recent advancements in large pretrained models have led to efforts to incorporate them into FL. FedKTL [46] introduced a knowledge-distillation-based method, that transfer distilled prototypes or representations to clients, addressing the challenges in knowledge transfer caused by data and model heterogeneity. In addition, AugFL [47] devised an inexact-ADMM-based algorithm for pretrained model personalized FL, allowing knowledge transfer from a private pretrained model at the server to clients while reducing computational cost. However, sharing pretrained model parameters or representations poses risks to the ownership of the these parameters [48]. Furthermore, transferring additional parameters or representations to clients may increase their computational and storage requirements. While bi-level optimization is utilized to train federated graph models with linear transformation layers and graph convolutional networks in BiG-Fed [49], this approach does not consider the non-IID degrees of the distributed data to future improve the accuracy of FL.

Finally, multiple methods address the heterogeneous computation and communication capacity of devices in FL. As an efficient method to reduce overfitting and achieve excellent performance, dropout [20] is exploited to reduce the communication and computation costs. Federated Dropout was proposed by extending this approach, which reduces communication costs by deriving small sub-models from the global model for local updates and exchanging only these sub-models between the servre and clients. However, dropout may incur accuracy degradation with an improper dropout rate [23]. While empirical experience may help set the dropout rate, the diversity of models and datasets brings difficulties in FL. Furthermore, a simple assessment of the dropout strategy based on the variation of loss values [22] does not consider the nature loss reduction within the FL training process and may correspond to low efficiency or low accuracy. Adaptive Federated Dropout maintains an activation score map to generate suitable sub-models for each client, enabling participation from clients with limited capabilities. However, it falls short in providing customized pruned sub-models tailored to different clients' specific needs. An ordered dropout mechanism is introduced to achieve ordered and nested representations of multiple models [21], which exploits a dropout rate space. However, the dropout rate space is still difficult to construct. Pruning methods are exploited to reduce the communication and computation costs [50, 51], which incur lossy operations and may degrade the accuracy.

4 System Model & Problem Formulation

In this section, we present our system model and formally formulate the problem we address.

System model. During the training process of FedDHAD, the global model is updated with multiple rounds. As shown in Figure 1, each round is composed of five steps. Within each round, the server randomly selects $N' = N * C$ devices, where C represents the ratio between the number of the selected devices and N . In Step ①, dropout operations are carried out and N' sub networks (subnet) are generated (see details in Section 5.2). The dropout rates of each device are updated when certain conditions are met (see details in Section 5.2). Then, the sub neural networks are downloaded to the selected devices through receiving the current global model parameters from the server in Step ②. Afterward, each selected devices then performs local computation based on the local dataset (see details in Section 5.1) in Step ③, and the updated model is uploaded to the server in Step ④. Finally, the updated models are aggregated with the consideration of the data heterogeneity in Step ⑤. While the model aggregation with the consideration of the data heterogeneity (see details in Section 5.1) introduces slight computation overheads, we exploit adaptive dropout (see details in Section 5.2) to accelerate the training process.

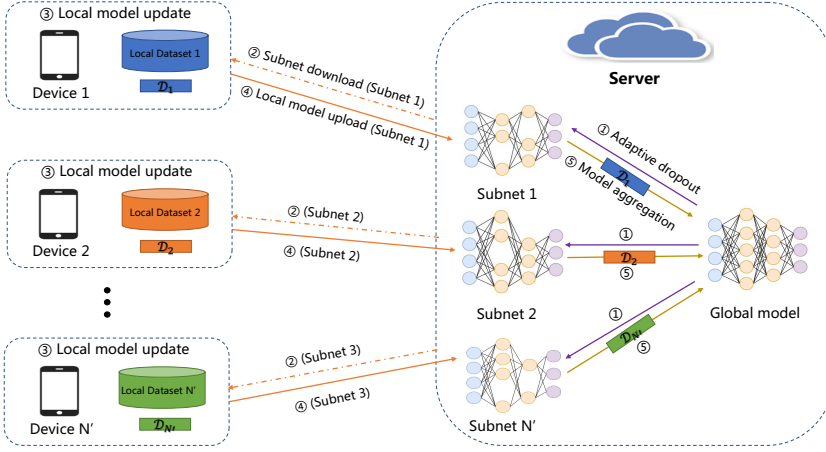


Fig. 1. The system model of FedDHAD.

Problem formulation. The problem to address in this paper is how to efficiently train a global model of high performance with a FL setting. We break down the problem into two aspects, *i.e.*, model performance and training efficiency. Thus, the first problem is how to achieve high model performance (defined in Formula 1) while considering the data heterogeneity. As data heterogeneity is critical to the model performance, the model performance problem consists of how to estimate non-IID degrees and how to leverage the non-IID degree to dynamically adjust the importance (weight) of each model. We formulate the training efficiency problem as how to minimize the training time of each round with heterogeneous devices while ensuring the performance of the trained model.

5 Efficient Heterogeneous FL with FedDHAD

In this section, we present the framework of FedDHAD. We first propose the dynamic heterogeneous model aggregation method, *i.e.*, FedDH. Then, we present the adaptive dropout method, *i.e.*, FedAD, to reduce the communication and computation costs in order to accelerate the training process while achieving excellent accuracy with heterogeneous devices. Then, we present the integration of the dynamic heterogeneous model aggregation method, *i.e.*, FedDH and the adaptive dropout method, *i.e.*, FedAD.

5.1 Heterogeneous Model Aggregation

In this section, we propose our dynamic heterogeneous federated learning method, *i.e.*, FedDH, which exploits the non-IID degrees of the heterogeneous data on each device to adjust the weights of multiple models in order to address the model performance problem. We first introduce a dynamic method to estimate the non-IID degree. Then, we present the details of FedDH. Afterward, we provide the theoretical convergence analysis of FedDH.

In order to address the model performance problem, we reformulate Formula 1 as a bi-level optimization problem [18] as follows:

$$\min_{w, Q} \left[F(w, Q) \triangleq \frac{1}{n} \sum_{k=1}^N n_k F_k(w(Q)) \right], w(Q) = \sum_{k=1, q_k \in Q}^{N'} q_k w_k, \quad (3)$$

$$s.t. w_k = \arg \min_{w_k} F_k(w_k) \forall k \in \{1, \dots, N\},$$

$$Q = \arg \min_Q F(w, Q), \quad \sum_{q_k \in Q}^{N'} q_k = 1,$$

where w represent the parameters for the global model, Q represents the set of weights for each model. The global model is a combination of local models based on the weights w . q_k is the weight for Model w_k uploaded from Device k . F is the loss function, which is defined in Section 2. F_k corresponds to the local loss function defined in Section 2. We perform the outer level optimization of Q to minimize F by dynamically updating weights using the estimated non-IID degrees. We conduct the inner optimization of local models to minimize the local loss function.

5.1.1 Non-IID Degree Estimation. While it is complicated to estimate the non-IID degree of the heterogeneous data, we propose a dynamic method to estimate the non-IID degree. A higher non-IID degree indicates a more significant difference in the data distribution between a device and that of all the overall dataset. While the Jensen–Shannon (JS) divergence [16] can be exploited to represent the non-IID degrees, there is still a slight difference between the JS divergence and the real non-IID degree of each device. Thus, we introduce extra control parameters, *i.e.*, $v_k \in \Upsilon$ and $b_k \in B$, where Υ and B represent the set of control parameters v_k and b_k , with the JS divergence for the non-IID degree representation as defined in Formula 4.

$$D_k^{non-IID}(P_k, v_k, b_k) = v_k \mathcal{D}_{JS}(P_k) + b_k, \quad (4)$$

where $D_k^{non-IID}(P_k, v_k, b_k)$ represents the non-IID degree of Device k . We exploit a linear transformation of JS divergence in Formula 4 while the parameters v_k and b_k are dynamically updated within FedDH based on Formula 10 to minimize the global loss function. We conduct experiments to empirically prove the linear relationship between JS divergence and non-IID degree. See details in Appendix. Based on Theorem 5.7, a proper representation of non-IID can lead to a better model. $\mathcal{D}_{JS}(P_k)$ represents the JS divergence of Device k as defined in Formula 5.

$$\mathcal{D}_{JS}(P_k) = \frac{1}{2} \mathcal{D}_{KL}(P_k || \bar{P}) + \frac{1}{2} \mathcal{D}_{KL}(P_m || \bar{P}), \quad (5)$$

where $\bar{P} = \frac{1}{2}(P_k + P_m)$, $P_m = \{P(y)|y \in \mathcal{Y}\} = \frac{\sum_{k=1}^N n_k P_k}{\sum_{k=1}^N n_k}$, $P_k = \{P(y)|y \in \mathcal{Y}_k\}$ with \mathcal{Y} representing the label set of the total dataset, \mathcal{Y}_k representing the label set of Dataset D_k , $P(y) = \{\theta_1, \theta_2, \dots, \theta_C\}$ representing the distribution of the corresponding dataset with θ_i referring to the proportion of data samples for Class i in Dataset D_k , and $\mathcal{D}_{KL}(\cdot || \cdot)$ is the Kullback-Leibler (KL) divergence [17] as defined in Formula 6:

$$\mathcal{D}_{KL}(P_i || P_j) = \sum_{y \in \mathcal{Y}} P_i(y) \log\left(\frac{P_i(y)}{P_j(y)}\right). \quad (6)$$

P_k values are statistical metadata of the raw data. The statistical meta information is similar (in terms of privacy issue) to the number of samples in each device, which is transferred to the server in standard FL, *e.g.*, FedAvg. As the statistical meta information reveals negligible privacy concerns and reveals negligible privacy concerns [52–54], we assume that P_k can be directly transferred from each device to the server in this paper.

When the statistical meta information cannot be directly transferred due to privacy issues, we can exploit the gradients from each device to estimate P_k , *i.e.*, FedDHE, which leads to similar performance as that of FedDH. Please note this is a complementary method when high security or privacy requirement is needed. In this case, we assume that there is a small dataset with a balanced class distribution on the server, which can be obtained from public data [55]. While sensitive data are not allowed to be transferred to the server, some insensitive data may reside in the servers or the cloud [55], which can be exploited as the small datasets on the server [56, 57]. The size of the balanced dataset is the same for each class. Please note that the balanced dataset cannot be exploited to train a satisfactory global model due to limited information. For each updated model from Device

Algorithm 1 Dynamic Heterogeneous Federated Learning (FedDH)**Input:** T : The maximum number of rounds N : The number of devices $P = \{P_1, P_2, \dots, P_N\}$: The set of the distribution of the data on each device $\lambda = \{\lambda_1, \lambda_2, \dots, \lambda_T\}$: The learning rates of control parameter update $H = \{\eta_1, \eta_2, \dots, \eta_T\}$: The learning rates of model update**Output:** w^t : The global model at Round t

- 1: **for** k in $\{1, 2, \dots, N\}$ (in parallel) **do**
- 2: Calculate $\mathcal{D}_{JS}(P_k)$ according to Formula 5; $v_k^0 \leftarrow 1$; $b_k^0 \leftarrow 0$
- 3: **end for**
- 4: **for** t in $\{1, 2, \dots, T\}$ **do**
- 5: Sample clients $C \subseteq \{1, 2, \dots, N\}$
- 6: **for** k in C **do**
- 7: Update w_k^t according to Formula 9 on each device
- 8: **end for**
- 9: Update w^t according to Formula 3
- 10: Update Υ^t and B^t according to Formula 10
- 11: Update Q according to Formula 11
- 12: **end for**

k , we can calculate the loss $L_i(w_k)$ with respect to Class i , and its corresponding gradients $\nabla L_i(w_k)$, based on the balanced dataset. We denote the set of gradients for C classes as:

$$\nabla L(w_k) = \{\nabla L_1(w_k), \nabla L_2(w_k), \dots, \nabla L_C(w_k)\}. \quad (7)$$

Inspired by [58], we estimate the proportion of data samples for Class i on Device k as:

$$\theta_k(i) = \frac{e^{\frac{\|\nabla L_i(w_k)\|^2}{\beta}}}{\sum_{j \in C} e^{\frac{\|\nabla L_j(w_k)\|^2}{\beta}}} \quad (8)$$

where β is a hyper-parameter to adjust the proportion normalization between each class. Then, we can obtain the estimated P_k . This process is performed once at the beginning of the training process.

5.1.2 Dynamic Heterogeneous Model Aggregation. During the training process of FedDH, the models and the control parameters are updated iteratively. The local model is updated on each device using the Stochastic Gradient Descent (SGD) approach as defined in Formula 9 [59], where t is the index of the round, $\nabla_{w_k^t} F_k(w_k^t)$ refers to the partial derivative of the model with respect to w_t on Device k , η^t represents the learning rate of the local training process on Device k . The model on each device can be a sub network generated from the global model (see details in Section 5.2).

$$w_k^{t+1} \leftarrow w_k^t - \eta^t \nabla_{w_k^t} F_k(w_k^t). \quad (9)$$

The control parameters are updated on the server using Formula 10, where λ_Υ^t and λ_B^t represent the learning rates for the update of Υ^t and B^t , respectively, $w^t(Q^t)$ is defined in Formula 3. $\nabla_{\Upsilon^t} F(w^t(Q^t))$ and $\nabla_{B^t} F(w^t(Q^t))$ refer to the partial derivative of the global model with respect to control parameters Υ^t and B^t , respectively, which can be calculated based on the sub network of each device.

$$\begin{aligned} \Upsilon^t &\leftarrow \Upsilon^t - \lambda_\Upsilon^t \nabla_{\Upsilon^t} F(w^t(Q^t)), \\ B^t &\leftarrow B^t - \lambda_B^t \nabla_{B^t} F(w^t(Q^t)), \end{aligned} \quad (10)$$

Then, the set of weights Q^t is updated based on Formula 11, where $D_k^{non-IID}(P_k, v_k^t, b_k^t)$ is defined in Formula 4. Formula 11 can incur higher accuracy with smaller loss compared with traditional aggregation methods (see theoretical analysis in Section 5.1.3). During the training process, we

calculate $\nabla_{\Gamma^t} F(w^t(Q^t))$ and $\nabla_{B^t} F(w^t(Q^t))$ only based on the selected devices (S^t) instead of all the devices.

$$q_k^t = \frac{\overline{D_k^{non-IID}(P_k, v_k^t, b_k^t)}^{n_k}}{\sum_{k \in S^t} \overline{D_k^{non-IID}(P_k, v_k^t, b_k^t)}^{n_k}}, \quad (11)$$

$$q_k^t \in Q^t, \forall k \in \{1, \dots, N\}.$$

FedDH is shown in Algorithm 1. First, the JS divergence is calculated and the control parameters are initialized (Lines 1 - 3). Then, the models are updated on each selected devices (Lines 5 - 8). Afterward, the global model (Line 9) the control parameters (Lines 10 - 11) are updated. Please refer to [60, 61] for the convergence proof of the bi-level optimization of control parameters and the models.

5.1.3 Theoretical Analysis. In this section, we present the theoretical convergence proof of FedDH. We first introduce the assumptions and then present the convergence theorems with an upper bound.

Assumption 5.1. *Lipschitz Gradient:* The function F_k is L -smooth for each device $k \in \mathcal{N}$ i.e., $\|\nabla F_k(x) - \nabla F_k(y)\| \leq L \|x - y\|$.

Assumption 5.2. μ -strongly convex: The function F_k is μ -strongly convex for each device $k \in \mathcal{N}$ i.e., $\langle \nabla F_k(x) - \nabla F_k(y), x - y \rangle \geq \mu \|x - y\|^2$.

Assumption 5.3. *Unbiased stochastic gradient:* $\mathbb{E}_{\zeta_{t,h}^k \sim \mathcal{D}_i} [\nabla f_k(w; \zeta_{t,h}^k)] = \nabla F_k(w)$.

Assumption 5.4. *Bounded local variance:* For each device $k \in \mathcal{N}$, the variance of its stochastic gradient is bounded: $\mathbb{E}_{\zeta_{t,h}^k \sim \mathcal{D}_i} \|\nabla f_k(w, \zeta_{t,h}^k) - \nabla F_k(w)\|^2 \leq \sigma^2$.

Assumption 5.5. *Bounded local gradient:* For each device $k \in \mathcal{N}$, the expected squared of stochastic gradient is bounded: $\mathbb{E}_{\zeta_{t,h}^k \sim \mathcal{D}_i} \|\nabla f_k(w, \zeta_{t,h}^k)\|^2 \leq G^2$.

When Assumptions 5.1 - 5.5 hold, we get the following theorem.

Theorem 5.6. *Suppose that Assumptions 5.1 to 5.5 hold and that the devices are with unbiased sampling. When the learning rate meets $\eta_{t,h} \leq \min\{\frac{1}{\mu}, \frac{1}{4L}\}$ for any t and h , then for all $R \geq 1$ we have:*

$$E \|F(w_{T,H}) - F(w^*)\| \leq \frac{L}{2} \frac{v}{TH + \gamma},$$

where $\gamma > 0$, $v = \max\{(\gamma + 1) \|\bar{w}_{1,1} - w^*\|, \frac{\beta m^2 B}{\beta \mu - 1}\}$, $\beta > \frac{1}{\mu}$, $B = 6L\Gamma + 2Q^2(H - 1)^2 \frac{G^2}{b} + \frac{\sigma^2}{b}$, $\Gamma = \max_{t \in \{1, \dots, T\}} \sum_{k \in S_t} p_{k,t} \Gamma_{k,t}$.

PROOF. See details in Appendix. \square

From Theorem 5.6, we can see that FedDH can converge when Assumptions 5.1 to 5.5 hold. In addition, as FedDH dynamically updates the control parameters to adjust the weight of each updated model, the upper bound of the distance between the global model and the optimal model is smaller compared with other baseline methods without dynamic update based on Theorem 5.7. As a result, the training efficiency of FedDH can be higher compared with the baseline methods.

Theorem 5.7. *Suppose that Assumptions 5.1 to 5.5 hold and that the devices are with unbiased sampling. When the conditions in Theorem 5.6 are met and the weights $p_{k,t} = \frac{\frac{n_k}{\bar{\Gamma}_{k,t}}}{\sum_{k' \in S_t} \frac{n_{k'}}{\bar{\Gamma}_{k',t}}}$, the upper bound of $E \|F(w_{T,H}) - F(w^*)\|$ is equal or smaller than that when $p_{k,t} = \frac{n_k}{\sum_{k' \in S_t} n_{k'}}$, with $(\gamma + 1) \|\bar{w}_{1,1} - w^*\| \leq \frac{\beta m^2 B}{\beta \mu - 1}$.*

Algorithm 2 Federated Adaptive Dropout (FedAD)**Input:**

- t : The current round
- w^* : The current global model at Round t
- FL : The list of fully connected layers in w^*
- CL : The list of convolutional layers in w^*
- S^t : The set of selected devices at Round t
- \mathcal{K} : The set of all devices
- SD^t : The set of selected devices for the pruning rates

Output:

- $w'^t = \{w'_k | k \in S^t\}$: The sub models at Round t
- 1: **if** should update dropout rates **then**
 - 2: **for** $k \in SD^t$ (in parallel) **do**
 - 3: $R_k^t = \{r_{k,l}^t | l \in CL \cup FL\} \leftarrow$ calculate the rank (weight) of each Filter (Neuron) i for each Layer l
 - 4: Calculate the dropout rate d_k using w^*
 - 5: **end for**
 - 6: Estimate ET_{max} using pruning rates
 - 7: Calculate aggregated R^t
 - 8: **for** $k \in \mathcal{K}$ (in parallel) **do**
 - 9: $d_k^* \leftarrow$ calculate the proper dropout rate using ET_{max}
 - 10: **for** $node^i \in CL$ or FL **do**
 - 11:
$$d_k^i = \frac{e^{-r_k^{t,i}}}{\sum_{j \in CL \text{ or } FL} e^{-r_k^{t,j}}} N_{CL \text{ or } FL} d_k^*$$
 - 12: **end for**
 - 13: **end for**
 - 14: **end if**
 - 15: **for** $k \in S^t$ (in parallel) **do**
 - 16: **for** $node^i \in CL \cup FL$ **do**
 - 17:
$$m_k^{i,t} = \begin{cases} \frac{1}{1 - d_k^i}, w.p. (1 - d_k^i), \\ 0, w.p. d_k^i \end{cases}$$
 - 18: **end for**
 - 19: $w'^t \leftarrow$ generate the sub model using the mask variables
 - 20: **end for**

PROOF. See details in Appendix. □

5.2 Federated Adaptive Dropout

In this section, we propose a neuron-adaptive dropout method, *i.e.*, FedAD, to address the training efficiency problem. FedAD dynamically generates adaptive sub models, which are adapted to the various characteristics and importance of neurons, for each device while achieving excellent accuracy with multiple heterogeneous devices. FedAD simultaneously reduces the computation costs on devices and the communication costs between devices and the server. We first present the details of FedAD. Then, we explain the model aggregation in FedDHAD, which combines FedDH and FedAD.

5.2.1 Adaptive Dropout. As shown in Algorithm 2, FedAD is composed of two parts, *i.e.*, dropout rate update (Lines 1 - 14) and model dropout operation (Lines 15 - 20). The dropout rate update is

computationally intensive, so we only perform it when model variation indicates the need for an update. The variation of the model is calculated every fixed rounds using euclidean distance equation $\Delta^t = \sqrt{(R^t - R^{t-h})^2}$. R^t is the set of the rank values and weights at Round t . The rank values of each filter are calculated based on the feature maps (outputs of filters) of filters [62], and the weight of each neuron is calculated as the sum of its corresponding input parameters in the model. The rank values and weights can well represent the importance of filters/neurons as they may have various impact on the output of the model [62]. The dropout rate is updated once there is no decrease in variation after \mathcal{C} rounds to avoid accuracy degradation in critical learning periods [63]. Additionally, the update is performed again when a reduction in variation is observed at a specific round.

Within the dropout rate update process, the rank value or the weight (Line 3) of each filter or neuron and the dropout rate (Line 4) of the global model is calculated cross selected devices SD . For each Device k , after t rounds of training, the parameters are updated to W'_k from the initial parameters W_k and the difference is denoted $\Delta_k = W_k - W'_k$. To capture the behavior of the local loss function, we calculate the Hessian matrix of the local loss function, i.e., $H(W'_k)$, with the eigenvalues sorted in ascending order, i.e., $\{\mathcal{E}_k^m | m \in (1, h_k)\}$, where h_k represents the rank of the Hessian matrix and m refers to the eigenvalue index. Next, We construct a function $B_k(\Delta_k) = H(W'_k) - \nabla L(W_k)$, where $\nabla L(\cdot)$ is the gradient of the local loss function. We denote the Lipschitz constant of $B_k(\Delta_k)$ by \mathcal{L}_k . To avoid possible accuracy degradation [64], we select the first eigenvalue m_k that satisfies the condition $\mathcal{E}_{m_{k+1}} - \mathcal{E}_{m_k} > 4\mathcal{L}_k$. Then, we calculate the dropout rate $d_k = \frac{m_k}{h_k}$. Afterward, we can calculate the aggregated dropout rate for the devices by $d_{avg} = \sum_{k \in SD} \frac{n_k}{\sum_{k \in SD} n_k} d_k$, which serves as the dropout rate on the device with the most significant dataset. We can get the execution time $ET_{max} = ET_{max}^o * d_{avg}$ of this device (Line 6), with ET_{max}^o representing the execution without dropout based on previous profiling information. Furthermore, we aggregate the rank values using $R^t = \sum_{k \in SD} \frac{n_k}{\sum_{k \in SD} n_k} R_k^t$ (Line 7). With this, the appropriate dropout rate for each device is recalculated as $d_k^* = \min\{\frac{ET_{max}^o}{ET_k^o}, 1\}$ (Line 9). The dropout rate of each filter or neuron d_k^i is then updated based on its rank values or weights $r_k^{t,i} \in R^t$ (Lines 10 - 12). In Line 11, $N_{CL \text{ or } FL}$ represents the number of filters or neurons in all convolutional layers CL or fully connected layers FL . Please note that the update operation (Lines 10 - 12) is carried out separately for convolutional layers and fully connected layers.

Finally, we perform the dropout operation with the updated dropout rates (Lines 15 - 20). The mask variables $m_k^{i,t}$ are calculated based on the probability d_k^i (Line 17). Within the dropout operation, when $m_k^{i,t} = 0$, the filter or the neuron is removed, and otherwise, the weight is updated (Line 19). In addition, while FedAD is primarily discussed in the context of traditional neural network architectures, it is designed to be adaptable and extendable to a variety of model types, including Transformers. The key principles of FedAD-adaptation of dropout rates base on model characteristics-are not inherently limited to convolutional layers or fully connected networks. In the case of Transformers, FedAD can be applied to dense layers and self/cross multi-head attention layers. Specifically, the adaptive dropout mechanism can selectively deactivate neurons in dense layers or individual attention heads based on their computed importance scores. By targeting these components, the method maintains computational efficiency while preserving the overall integrity and performance of the model.

FedAD updates the dropout rates of each filter or neuron based on its rank values or weights, determining which filters or neurons in each layer should be dropped out with certain possibility. Within the dropout operation, when $m_k^{i,t} = 0$, the filter or the neuron is removed, and otherwise, the weight is updated (Line 19). The dropout operation of a layer l is a special case, i.e., $m_k^{i,t} = 0$ for $i \in \text{Layer } l$. Although this may be efficient in calculating the dropout rate, it may bring significant accuracy degradation due to the absence of a whole layer.

5.2.2 Model Aggregation. In order to aggregate the heterogeneous models, we take an efficient model aggregation method in FedDHAD. For the neurons or filters that are not removed (dropped) in all the selected devices, we directly exploit Formula 3 to calculate the aggregated value as follows: $m^i = \sum q_k * m_k^i$, where m^i represents the parameter in the global model, q_k^i represents the weight of Model k in Q and m_k^i represents the parameter in local Model k . If the neurons or filters are removed (dropped) in Set Drop, we calculate the aggregated weight based on the following formula: $m^i = (\sum_{k \notin Drop} q_k * m_k^i) / (\sum_{k \notin Drop} q_k)$, which is the sum of the valid weighted parameters (the corresponding filter or neuron is not dropped on the devices) divided by the sum of weights corresponding to the devices of valid parameters (the corresponding filter or neuron is not dropped on the devices).

5.3 The Integration of FedDH and FedAD

In this section, we detail the integration of the proposed methods FedDH and FedAD into FedDHAD framework. The FedDHAD framework synergistically combines the strengths of FedDH and FedAD to addresses both the model performance and training efficiency problems inherent in FL with non-IID data distributions and heterogeneous devices.

Specifically, during each training round in FedDHAD, the server begins by performing the neuron-adaptive dropout mechanism of FedAD to generate sub-models for the selected devices. The dropout rates for each filter or neuron are dynamically adjusted based on the importance of filters or neurons and the resource constraints of the device. The generated sub-models are then distributed to the selected devices, where local training is conducted using their respective local datasets. After local training, the devices upload their updated sub-models back to the server. The server then performs dynamic heterogeneous model aggregation using the FedDH method, which exploits the non-IID degrees of the heterogeneous data on the selected devices to adjust the aggregation weights. The integration offers synergistic benefits. The slight computational overhead introduced by FedDH is effectively compensated by the efficiency gains from FedAD, resulting in accelerating the training process and improving model accuracy.

The integration of FedDH and FedAD into the FedDHAD framework establishes a synergistic relationship that simultaneously addresses statistical data heterogeneity and device heterogeneity in FL. While both methods demonstrate effectiveness independently, their combination yields complementary advantages. FedDH addresses model performance challenges through dynamic weight adjustment based on non-IID degrees, while FedAD optimizes communication and computation efficiency via adaptive dropout operations. The computational overhead introduced by the dynamic weight calculations of FedDH is compensated by the efficiency gains from the reduced model size of FedAD. Furthermore, the weighted aggregation mechanism of FedDH mitigates potential accuracy degradation from the dropout operations of FedAD by appropriately valuing the contribution of each device according to its data distribution characteristics. Additionally, the resource optimization of FedAD enables more training rounds within constrained time budgets, providing FedDH with increased opportunities to refine weight adjustments. Thus, the combination of these two approaches in FedDHAD yields superior performance in terms of both accuracy and efficiency compared to either method individually or state-of-the-art baseline approaches.

6 Experimental Evaluation

In this section, we compare FedDHAD with 13 state-of-the-art baseline approaches, exploiting four models and four datasets. We choose baseline methods that specifically address data and device heterogeneity challenges in FL. We includes methods (e.g. FedAvg [7], FedProx [15], and FedNova [10]) which set foundational standards for handling non-IID data, alongside recent advancements (e.g.

Table 3. Performance comparison on CIFAR-10 and CIFAR-100 datasets. FedDHAD, FedDH, and FedAD are our proposed methods. The best results are highlighted in **bold** and the second best results are highlighted with underline and *italic*.

Method	CIFAR-10						CIFAR-100					
	LeNet			CNN			LeNet			CNN		
	Acc	Time	MLPs									
FedDHAD (ours)	0.633	1371	0.618	0.749	3074	4.324	0.300	2127	0.609	0.423	4952	4.416
FedDH (ours)	<i>0.621</i>	1426	0.652	<i>0.744</i>	<i>3322</i>	4.549	<i>0.297</i>	2495	0.659	<i>0.420</i>	<i>5018</i>	4.554
FedAD (ours)	0.595	<i>1394</i>	0.615	0.732	3632	4.324	0.295	<i>2175</i>	0.604	0.412	5324	4.330
FedAvg	0.565	2366	0.652	0.730	5265	4.549	0.263	5714	0.659	0.414	5089	4.554
FedProx	0.588	1994	0.652	0.730	3912	4.549	0.274	3750	0.659	0.415	5613	4.554
FedNova	0.582	2200	0.652	0.728	5296	4.549	0.286	3082	0.659	0.416	5514	4.554
MOON	0.610	2871	0.689	0.741	4513	4.584	0.281	3682	0.712	0.405	7031	4.628
FedDyn	0.543	2256	0.652	0.700	NaN	4.549	0.228	NaN	0.659	0.344	NaN	4.554
FedDST	0.582	2178	0.645	0.645	NaN	4.504	0.168	NaN	0.652	0.181	NaN	4.508
PruneFL	0.392	NaN	0.652	0.524	NaN	4.549	0.127	NaN	0.659	0.187	NaN	4.554
AFD	0.511	3909	0.637	0.589	NaN	4.540	0.270	3768	0.644	0.228	NaN	4.550
FedDrop	0.585	3993	0.636	0.725	5385	4.533	0.254	NaN	0.640	0.405	6540	4.538
FjORD	0.593	1663	0.482	0.723	4556	3.474	0.292	2262	0.489	0.369	NaN	3.479
MOON+FjORD	0.608	2821	<i>0.526</i>	0.737	4609	<i>3.959</i>	0.288	3376	<i>0.518</i>	0.416	5424	<i>4.043</i>

MOON [25], FedDyn [24], FedAS [65], FedKTL [46] and AugFL [47]). We selected methods (e.g. FedDST [51], PruneFL [50], AFD [22], FedDrop [23], and FjORD [21]) for device heterogeneity. Additionally, we integrated combinations (e.g. MOON and FjORD), ensuring a comprehensive and fair comparison. First, we present the experimental setup. Then, we present our experimentation results.

6.1 Experimental Setup

We consider a standard FL environment composed of a server and 100 devices, each with its stored data, and we randomly select 10 devices in each round. We simulate this environment using 44 Tesla V100 GPU cards. We use the datasets of CIFAR-10[66], CIFAR-100 [66], SVHN [67], and TinyImageNet [68]. We report the results of four models, i.e., a simple synthetic CNN network (CNN), LeNet5 (LeNet) [69], VGG11 (VGG) [70], and ResNet18 (ResNet) [71]. The complexity of the four models are: ResNet (11,276,232 parameters) > VGG (9,750,922 parameters) > CNN (122,570 parameters) > LeNet (62,006 parameters). We utilize a decay rate in both the training process of devices and the control parameter adjustment. We take 500 as the maximum number of rounds for LeNet, CNN, and VGG and 1000 as that for ResNet. We fine-tune the hyper-parameters and present the best performance for each approach. The accuracy, the training time to achieve target accuracy, and the computation costs are shown in Tables 3 and 4. We report the training time (s) to achieve the specific accuracies. These target accuracies were selected based on empirical observations of the training process and represent points where the models demonstrate significant learning progress while still having room for further improvement. Instead of using a predefined standard, such as the average accuracy of all methods or a fraction of the accuracy of the best method, these specific values were chosen to provide a clear and practical benchmark for comparing the convergence speeds of different methods.

We exploit four datasets including CIFAR-10 (60,000 images with 10 classes), CIFAR-100 (60,000 images with 100 classes), SVHN (99289 images with 10 classes), and TinyImageNet (100,000 images with 200 classes). We allocate each device a proportion of the samples of each label according to Dirichlet distribution [13]. Specifically, we sample $p_k \sim Dir(\beta)$ and allocate a proportion of the samples in class k to Device j . $Dir(\beta)$ is the Dirichlet distribution with a concentration parameter β (0.5 by default), the values of which corresponds to various non-IID degrees of the data in each device. We exploit the same method to handle the other datasets. We use a learning rate of 0.1 for

Table 4. Performance comparison on SVHN and TinyImageNet datasets. “Time*” represents $\times 10^2$ s. FedDHAD, FedDH, and FedAD are our proposed methods. The best results are highlighted in **bold** and the second best results are highlighted with underline and *italic*.

Method	SVHN									TinyImageNet		
	LeNet			CNN			VGG			ResNet		
	Acc	Time	MLPs	Acc	Time	MLPs	Acc	Time*	MLPs	Acc	Time*	MLPs
FedDHAD (ours)	0.8760	1645	0.620	0.9110	1177	<i>4.127</i>	0.9367	131	138.9	0.3765	859	474.3
FedDH (ours)	<i>0.8755</i>	<i>1777</i>	0.652	<i>0.9093</i>	<i>1228</i>	4.549	<i>0.9321</i>	<i>132</i>	153.3	0.3724	1003	558.0
FedAD (ours)	0.8665	2246	0.615	0.9056	1650	4.172	0.9309	141	139.4	<i>0.3763</i>	615	<i>472.3</i>
FedAvg	0.8663	2347	0.652	0.9055	1595	4.549	0.9286	154	153.3	0.3638	1276	558.0
FedProx	0.8652	2374	0.652	0.8999	1864	4.549	0.9260	159	153.3	0.3694	1256	558.0
FedNova	0.8663	2333	0.652	0.9023	1454	4.549	0.9287	149	153.3	0.3598	1579	558.0
MOON	0.8550	4843	0.689	0.8849	3558	4.584	0.1870	NaN	153.2	0.1536	NaN	558.0
FedDyn	0.8338	NaN	0.652	0.8813	2174	4.549	0.1646	NaN	153.3	0.0792	NaN	558.0
FedDST	0.8554	2774	0.647	0.8845	1906	4.299	0.1851	NaN	148.7	0.3014	NaN	446.4
PruneFL	0.8450	NaN	0.652	0.8994	1668	4.549	0.1646	NaN	153.3	0.3322	NaN	558.0
AFD	0.8504	3185	0.648	0.5046	NaN	4.531	0.7683	NaN	152.9	0.3727	<i>761</i>	557.7
FedDrop	0.8568	3031	0.636	0.8985	1728	4.533	0.9285	170	152.3	0.3748	865	557.2
FjORD	0.8434	2185	0.482	0.900	1730	3.959	0.9107	154	116.5	0.3463	NaN	489.7
MOON+FjORD	0.8414	NaN	<i>0.528</i>	0.8964	1765	4.279	0.1992	NaN	<i>118.4</i>	0.1456	NaN	536.4

the model update, a learning rate decay of 0.99 for the model update, a batch size of 10, and a local epoch (τ) of 5. The values of the other hyper-parameters are shown in Table 5.

The accuracy and training time with FedDH, FedAD and various baseline methods for LeNet and CNN with CIFAR-10 and CIFAR-100 are shown in Figure 2, and the results for LeNet, CNN, and VGG with SVHN and ResNet with TinyImageNet are shown in Figure 3. We adaptively attribute dropout rates for each filter and neuron, which yields stable performance. The results of accuracy and rounds are shown in Figures 4, which reveal FedDHAD corresponds to more stable training process than other methods.

We evaluate the performance of our proposed methods using three key metrics: accuracy, training time, and computation cost. Accuracy measures the proportion of correctly classified samples in the test dataset using the trained global model. Training time is measured in seconds (s) and represents the time required to achieve a target accuracy level, which varies by model and dataset combination. For CIFAR-10, we set target accuracies of 0.54 for LeNet and 0.72 for CNN; for CIFAR-100, 0.26 for LeNet and 0.41 for CNN; for SVHN, 0.85 for LeNet, 0.88 for CNN, and 0.91 for VGG; and for TinyImageNet, 0.36 for ResNet. Computation cost is measured in Million Floating Point Operations (MFLOPs), which quantifies the computational complexity of the model training process. This metric is calculated as the sum of all floating-point operations required for forward and backward passes during model training, divided by 10^6 . Lower MFLOPs values indicate more computationally efficient methods.

6.2 Evaluation of Our Approach

In this section, we present the experimental results for FedDH and FedAD. Then, we show the evaluation results of the combination of FedDH and FedAD, i.e., FedDHAD.

6.2.1 Evaluation of FedDH. In this section, we compare the accuracy of FedDH with FedAvg [7], FedProx [15], FedNova [10], MOON [25], FedDyn [24], FedAS [65], FedKTL [46] and AugFL [47]. FedDH dynamically adjusts the weights of uploaded models with the non-IID degree of the heterogeneous data in the model aggregation process, corresponding to superior performance. As shown in Table 3, FedDH achieves a significantly higher accuracy compared with FedAvg (5.6%), FedProx (3.3%), FedNova (4.0%), MOON (1.1%), and FedDyn (7.8%) for LeNet with CIFAR-10. We find that FedDyn leads to lower accuracy than FedAvg. Although FedNova, FedProx, and MOON

Table 5. Values of hyper-parameters in the experimentation. “TI” represents TinyImageNet.

Name		Values							
		LeNet			CNN			VGG	ResNet
		CIFAR-10	CIFAR-100	SVHN	CIFAR-10	CIFAR-100	SVHN	SVHN	TI
FedDH & FedAD	λ_γ	0.0001	0.01	0.01	0.001	0.001	0.01	0.001	0.1
	$decay_\gamma$	0.999	0.99	0.999	0.9999	0.9999	0.999	0.9	0.9
	λ_B	0.0001	0.1	0.01	0.1	0.0001	0.001	0.0001	0.1
	$decay_B$	0.99	0.99	0.99	0.99	0.99	0.99	0.999	0.999
FedDHAD	λ_γ	0.01	0.01	0.0001	0.0001	0.01	0.1	0.1	0.1
	$decay_\gamma$	0.9999	0.9999	0.999	0.999	0.9999	0.99	0.99	0.9999
	λ_B	0.0001	0.0001	0.1	0.1	0.0001	0.01	0.01	0.001
	$decay_B$	0.99	0.99	0.99	0.99	0.99	0.99	0.99	0.99

outperform FedAvg, they correspond to lower accuracy than FedDH due to simple model aggregation. In addition, we find similar results for CNN with CIFAR-10, while the advantages of FedDH (from 0.3% to 4.5%) are relatively smaller than those of LeNet. Furthermore, Table 3 reveals significant advantages (up to 3.4% for FedAvg, 2.3% for FedProx, 1.1% for FedNova, 2.2% for MOON, and 8.3% for FedDyn) of FedDH for LeNet and CNN with CIFAR-100. As shown in Table 4, we can observe that FedDH corresponds to much higher accuracy compared with FedAvg (up to 0.9%), FedProx (up to 1.0%), FedNova (up to 1.3%), MOON (up to 74.5%), and FedDyn (up to 76.8%) while dealing with SVHN and TinyImageNet.

6.2.2 Evaluation of FedAD. In this section, we present the comparison results between FedAD and FedAvg [7], Federated Dynamic Sparse Training (FedDST) [51], PruneFL [50], Adaptive Federated Dropout (AFD) [22], Federated Dropout (FedDrop) [23], and FjORD [21], in terms of both the accuracy and efficiency. We take the dropout rates of 0.25 for AFD as reported in [22] and 0.5 for FedDrop, which corresponds to the highest accuracy reported in [23]. In addition, we fine-tune the hyper-parameters of FjORD to achieve the best accuracy.

We find that the total training time of FedAD is much shorter than that of FedAvg (up to 8.6%), and FedDrop (up to 4.5%), AFD (up to 21.9%), but longer than that of FjORD (up to 27.6%). However, as shown in Table 3, the accuracy of FedAD is significantly higher than that of FedAvg (up to 3.2%), FedDrop (up to 4.1%), AFD (up to 18.4%), and FjORD (up to 4.3%) for LeNet and CNN with CIFAR-10 and CIFAR-100. In addition, FedAD leads to the shortest training time (up to 31.0% compared with FedAvg, up to 36.0% compared with FedDST, 55.1% compared with FedDrop, and 25.8% compared with FjORD) to achieve the target accuracy with LeNet (AFD and PruneFL cannot achieve the target accuracy) and corresponds to smaller computation costs compared with FedAvg (up to 8.6%), FedDST (up to 7.4%), PruneFL (up to 9.1%), AFD (up to 6.6%), and FedDrop (up to 4.5%) because of the adaptive dropout rates. We can get similar results on LeNet, CNN, and VGG over SVHN and ResNet over TinyImageNet as shown in Table 4. FedAD is designed to reduce the communication and computation costs in order to accelerate the training process while achieving excellent accuracy with heterogeneous devices. As shown in Table 3 and Table 4, the total training time of FedAD is much shorter than that of FedDH (up to 38.7%). While the total training time of FedDH is shorter sometimes, FedAD leads to consistent lower computation costs (up to 15.4%) compared with FedDH.

While the computation costs of FjORD are smaller compared with FedAD, FedAD leads to significantly higher accuracy (up to 4.3%). As FedDrop is only applied to the fully connected layers, it corresponds to a longer training time compared with AFD, FjORD, and FedAD. Since FedDrop only considers random dropout operation, its accuracy is slightly lower than that of FedAvg for both LeNet (up to 0.9%) and CNN (up to 0.5%). While AFD considers the influence of dropout on the loss, it ignores the phenomenon that the loss is naturally reduced during the training process and thus corresponds to significantly inferior accuracy (up to 18.4% compared with FedAD, 18.6% compared with FedAvg, and 17.7% compared with FedDrop). Although FjORD can adaptively tailor the model width for heterogeneous devices, it cannot achieve lossless pruning and corresponds to inferior accuracy (up to 4.3%) compared with FedAD. FedAD adaptively calculates the dropout

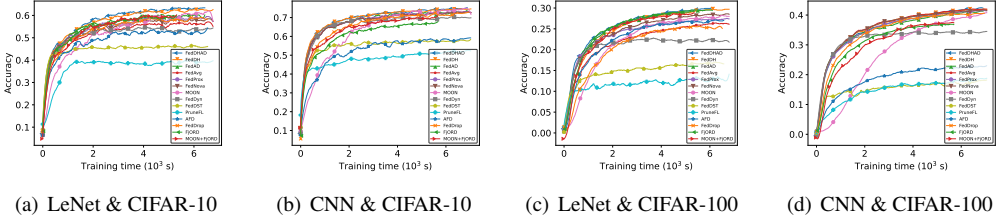


Fig. 2. The accuracy and training time with FedDHAD and various baseline methods for LeNet and CNN with CIFAR-10 and CIFAR-100.

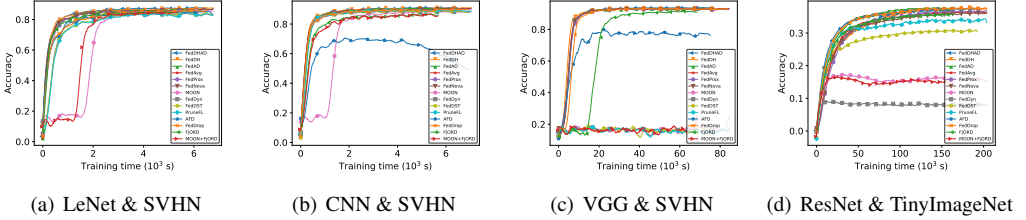


Fig. 3. The accuracy and training time with FedDHAD and various baseline methods for LeNet, CNN, and VGG with SVHN and ResNet with TinyImageNet.

rate, which leads to excellent final accuracy within a short training time. Notably, the use of VGG model in SVHN results in significantly lower accuracy, primarily due to the inherent complexity and the large number of parameters (e.g. 9,750,922 parameters) of VGG. This complexity makes VGG vulnerable to the challenges of data heterogeneity. Furthermore, PruneFL employs pruning methods that involve lossy operations, which can further degrade accuracy.

6.2.3 Evaluation of FedDHAD. In this section, we integrate FedDH and FedAD into FedDHAD, which we evaluate in comparison with FedAvg, FedProx, FedNova, MOON, FedDyn, FedAS, FedKTL, AugFL, FedDST, PruneFL, AFD, FedDrop, FjORD and a combination of MOON and FjORD, in terms of both accuracy and efficiency.

As shown in Tables 3 and 4, FedDHAD leads to high accuracy and fast convergence. The accuracy of FedDHAD is significantly higher than FedAvg (up to 6.7%), FedProx (up to 4.5%), FedNova (up to 5.1%), MOON (up to 74.5%), FedDyn (up to 76.8%), FedDST (up to 78.6%), PruneFL (up to 61.5%), AFD (up to 19.5%), FedDrop (up to 4.8%), FjORD (up to 4.7%) and the combination of MOON and FjORD (up to 8.9%) for LeNet, CNN, VGG, and ResNet, because of dynamic adjustment of control parameters and adaptive dropout operations. In addition, FedDHAD corresponds to the shortest training time (up to 1.69 times shorter compared with FedAvg, 43.3% compared with FedProx, 42.0% compared with FedNova, up to 2.02 times shorter compared with MOON, 45.9% compared with FedDyn, 40.7% compared with FedDST, 29.4% compared with PruneFL, 1.85 times compared with AFD, and 1.91 times compared with FedDrop, 32.5% compared with FjORD, and 51.4% compared with the combination of MOON and FjORD) to achieve target accuracy for LeNet, CNN, VGG, and ResNet. Although it corresponds to a slightly longer time to achieve the target time compared with AFD (0.47 times longer), FedDHAD leads to higher accuracy (0.2% compared with AFD) with ResNet. In addition, FedDHAD incurs smaller computation costs (up to 14.9% compared with FedAvg, FedProx, FedNova, FedDyn, and PruneFL, 15.0% compared with MOON, 10.1% compared with AFD, and 9.8% compared with FedDrop) than those presented above, while corresponding to slightly higher computation costs (up to 28.6%) than FjORD. In addition, the total training time of FedDHAD is shorter than that of FedAD (up to 28.7%). This is primarily because of the dynamic adjustment of the weights of local models, which corresponds to higher

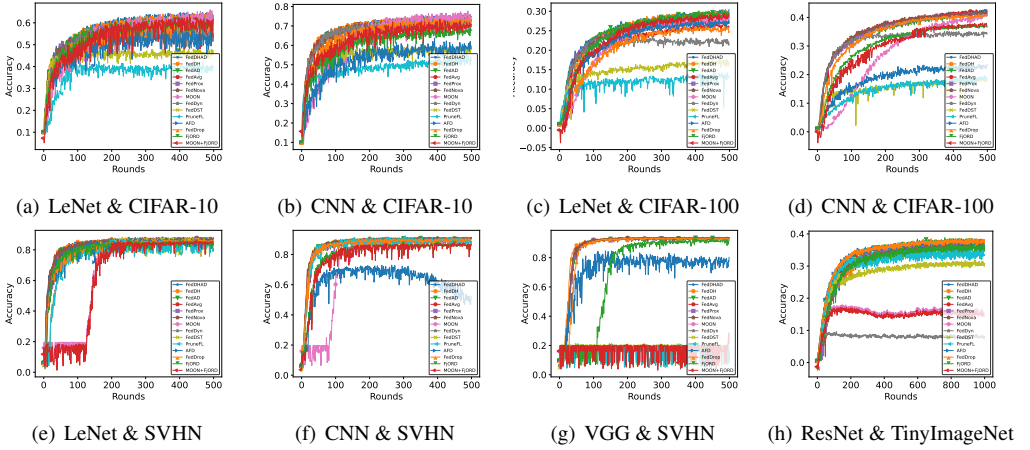


Fig. 4. The accuracy and training rounds with FedDHAD and various baseline methods for LeNet and CNN with CIFAR-10 and CIFAR-100, LeNet, CNN, and VGG with SVHN and ResNet with TinyImageNet.

accuracy. FedDHAD, by incorporating FedDH, adjusts the weights of local models during the model aggregation process based on the non-IID degrees of the heterogeneous data, achieving more efficient model aggregation and global model updates compared with FedAD. However, FedAD only performs the dropout rate update. The dropout rate update operation adjusts the dropout rates based on the rank or weight of filters and neurons, which can avoid performance degradation and exist in FedDHAD as well. Thus, the combination of FedDH and FedAD leads to a more efficient optimization process in FedDHAD compared to FedAD alone.

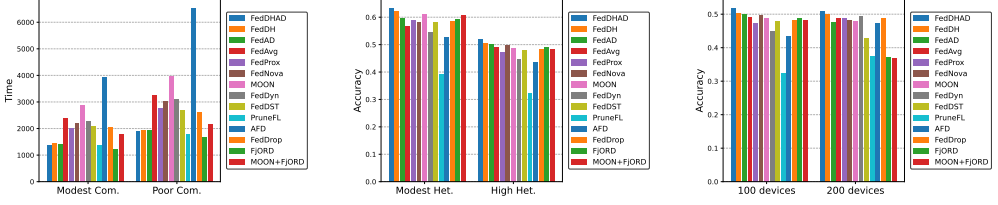
We carry out experiments to evaluate the performance of FedDHAD with various network bandwidth, various non-IID degrees of data, and different numbers of devices. When the network connection becomes worse, the advantages of FedDHAD become significant (from 64.9% to 82.7%) because of communication reduction brought by the adaptive dropout. As it can exploit the non-IID degrees of the data on each device to adjust the weights of multiple models, FedDHAD achieves superior accuracy (from 6.9% to 10.7%) even with the data of high non-IID degrees. Furthermore, FedDHAD incurs 13.5% higher accuracy and 8.6% shorter training time to achieve target accuracy with different numbers of devices and the significance becomes obvious with a large scale of devices.

6.3 Evaluation with various Environments

In this section, we give our experimental results performed with various environments along three dimensions: network bandwidth, statistical data heterogeneity and scalability in number of devices.

6.3.1 Network Bandwidth. While devices have limited network connection, we analyze the performance of FedDHAD with different bandwidths. As shown in Figure 5(a), when the bandwidth becomes modest, FedDHAD corresponds to significantly higher training speed (up to 64.9%) compared with baseline approaches. We observe FedDHAD corresponds to higher accuracy (up to 10.7%) compared with baseline approaches with the modest bandwidth as well. When the network connection becomes worse, the advantages of FedDHAD become significant (from 64.9% to 82.7%) because of communication reduction brought by the adaptive dropout.

6.3.2 Statistical Data Heterogeneity. As shown in Figure 5(b), when the device data is of high heterogeneity, i.e., high non-IID degree data, FedDHAD significantly outperforms other baseline approaches in terms of accuracy (up to 6.9%). In addition, we find FedDHAD leads to a shorter



(a) Time to target accuracy (0.54) under various bandwidths. “Com.” represents heterogeneity. “Het.” represents “Hetero- of devices. “Communication”.

Fig. 5. Performance of FedDHAD and various baseline methods with LeNet on CIFAR-10.

training time (up to 52.2%) to achieve the target accuracy compared with baseline approaches with the data of high non-IID degree, because of dynamic adjustment of control parameters and adaptive dropout operations. When the device data are highly heterogeneous, the advantage of FedDHAD corresponds to higher accuracy becomes obvious (from 6.9% to 10.7%). As it can exploit the non-IID degrees of the distributed data on each device to adjust the weights of multiple models, FedDHAD achieves superior accuracy with the data of high non-IID degrees.

6.3.3 Scalability. To show the scalability of FedDHAD, we carry out experiments with a large number (200) of devices with LeNet on CIFAR-10. The results are shown in Figure 5(c), FedDHAD significantly outperforms other baseline approaches in terms of accuracy (up to 13.5%). In addition, we find FedDHAD incurs a shorter training time (up to 8.6%) to achieve target accuracy with 200 devices compared with that of 100. Furthermore, we study the effect of the number of devices on multiple approaches as shown in Figure 5(c). As the number of devices increases, the amount of local data decreases. We observe that the accuracy of baseline approaches decreases significantly when increasing the number of devices (up to 11.6%). However, The advantages of FedDHAD become significant on a large-scale setting with small data in the device.

6.4 Evaluation of Single Methods

In this section, we further evaluate the single methods that contribute to the superiority of our approach. We first present the evaluation of our data distribution estimation method. Then, we give a comparison between FedDH and a static method. Afterward, we analyze the computation cost of FedDH (to update Q in Formula 3) on the server. Finally, we provide the ablation study corresponding to the contribution of FedDH and FedAD to FedDHAD.

6.4.1 Data Distribution Estimation. We carried out an experiment to verify the difference between FedDH and the data distribution estimation method without transferring meta information, i.e., FedDHE. As shown in Figures 6(a) and 6(b), we find that FedDH and FedDHE lead to similar accuracy (with the difference less than 0.8% for both LeNet and CNN). Thus, when the meta information is not allowed to be transferred from devices to the server for high privacy requirements, we can exploit FedDHE instead of FedDH.

6.4.2 Comparison with Static JS Divergence. To show that static JS divergence (FedJS) cannot well represent the non-IID degree, we carried out an experiment with LeNet and CNN on CIFAR-10, which reveals the difference between FedDH and FedJS. Figures 6(c) and 6(d) show that FedDH significantly outperforms FedJS in terms of accuracy (up to 2.9% for LetNet and 0.9% for CNN).

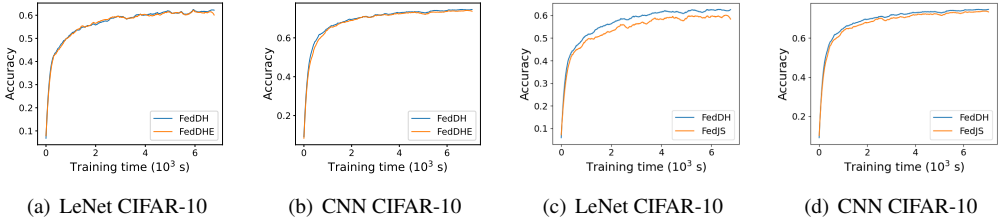


Fig. 6. The accuracy and training time with FedDH, FedDHE, and FedJS for LeNet and CNN on CIFAR-10.

6.4.3 Server Computation Overhead. As FedDHAD involves server computation, we quantify its overhead in terms of time. As shown in Table 2, the overheads of FedDH are up to 10.4%, which is quite small. In addition, the overheads of FedDHAD are up to 15.6%, which corresponds to higher accuracy, shorter time to achieve target accuracy, and smaller computation costs.

6.4.4 Ablation Study. In this section, we present the advantages of FedDH and FedDH, corresponding to the specific contribution to FedDHAD. As shown in Tables 3 and 4, FedDHAD can achieve higher accuracy and shorter training time to achieve the target accuracy compared with FedDH (up to 1.1% in terms of accuracy and 14.7% in terms of training time) and FedAD (up to 3.8% in terms of accuracy and 28.7% in terms of training time). As FedDHAD carries out the dynamic adjustment of the weights and the adaptive dropout operations at the same time, it leads to the shortest training time (up to 26.8%) to achieve target accuracy (except for TinyImageNet with ResNet) and corresponds to the same computation cost or slightly higher (up to 0.5%) for CIFAR-10, CIFAR-100, and SVHN, compared with FedAD. FedDH corresponds to higher accuracy compared with FedAD (up to 2.6%) and FedAD incurs smaller computation costs (up to 15.4%). FedDHAD corresponds to slightly higher computation costs compared with FedAD (up to 0.5%) because of FedDH. With ResNet and TinyImageNet, FedDHAD corresponds to the highest accuracy while FedAD incurs the shortest time to achieve the target accuracy and computational costs. When tight training budget is required and big models are exploited, FedAD can be exploited. Otherwise, FedDHAD can be selected.

7 Conclusion

In this paper, we proposed FedDHAD, an FL framework that simultaneously addresses statistical data heterogeneity and device heterogeneity. We proposed two novel methods: Dynamic Heterogeneous model aggregation (FedDH) and Adaptive Dropout (FedAD). FedDH exploits the non-IID degrees of devices to dynamically adjust the weights of each local model within the model aggregation process. FedAD adapts the dropout operation to each device while reducing communication and computation costs and achieving a good balance between efficiency and effectiveness. By combining these two methods, FedDHAD is able to adaptively calculate the dropout rates in each round with good load balancing, thus addressing the training efficiency problem, and dynamically adjusts the weights of the models with removed neurons, thus improving model accuracy.

The extensive experimental results reveal that FedDHAD significantly outperforms the state-of-the-art baseline approaches in terms of accuracy (up to 6.7% higher), efficiency (up to 2.02 times faster), and computation cost (up to 15.0% smaller). The experimental evaluation demonstrates as well that FedDHAD has significant advantages in various environments, e.g., modest network (FedDHAD is robust to bandwidth), high non-IID degree (FedDHAD is effective with heterogeneous data) and large number of devices (FedDHAD has excellent scalability).

Large Language Models (LLMs) have shown great potential in numerous tasks due to their large-scale pre-trained architectures. The training process of LLMs typically involves updating a

large number of parameters [72, 73], limiting the use of FL techniques in real-world scenarios. Future directions could explore using FedDHAD principles, focusing on efficient model updates and adaptive dropout tailored for LLMs. Additionally, future directions could explore improving the adaptivity of the FedDHAD framework by incorporating fine-grained control over dropout and model aggregation weights for extreme heterogeneity cases. By integrating personalized federated learning approaches, we can further ensure individual client needs are addressed, enhancing model performance across diverse data distributions. In addition, FedDHAD relies on central server for model aggregation. Future directions could extend to decentralized federated learning architectures, where model aggregation is performed collaboratively by participating devices. This shift could enhance robustness, reduce communication latency, and increase the resilience of system to server-side attacks or failures. By addressing these future directions, we aim to further the capabilities and applicability of federated learning, paving the way for more efficient, decentralized, and secure machine learning systems at scale.

Appendix

In this section, we present the theoretical convergence proof, the correlation between JS divergence and non-IID degree, and the limitations of FedDHAD.

Convergence Proof

We first introduce the assumptions and then present the convergence theorems with an upper bound.

PROOF. First we have

$$\begin{aligned} \|\bar{w}_{t,h+1} - w^*\| &= \underbrace{\|\bar{w}_{t,h} - \eta_{t,h}\bar{g}_{t,h} - w^*\|}_{A_1} + \underbrace{\|\eta_{t,h}\bar{g}_{t,h} - \eta_{t,h}g_{t,h}\|}_{A_2} \\ &\quad + 2 \underbrace{\langle \bar{w}_{t,h} - \eta_{t,h}\bar{g}_{t,h} - w^*, \eta_{t,h}\bar{g}_{t,h} - \eta_{t,h}g_{t,h} \rangle}_{A_3} \end{aligned}$$

Note that $E[A_3] = 0$ when devices are with unbiased sampling, bound A_1 :

$$A_1 = \underbrace{\|\bar{w}_{t,h} - w^*\|}_{B_1}^2 + \underbrace{\|\eta_{t,h}\bar{g}_{t,h}\|}_{B_2}^2 - 2\eta_{t,h}\langle \bar{w}_{t,h} - w^*, \bar{g}_{t,h} \rangle$$

By the convexity of $\|\cdot\|^2$ (Jensen's inequality) and L-smoothness of F_k ,

$$B_1 \leq 2L\eta_{t,h}^2 \sum_{k \in S_t} p_{k,t} (F_k(w_{t,h}^k) - E[F_k(w_k^*)])$$

Next, we bound B_2 :

$$\begin{aligned} B_2 &= -2\eta_{t,h} \sum_{k \in S_t} p_{k,t} \langle \bar{w}_{t,h} - w_{t,h}^k, \nabla F_k(w_{t,h}^k) \rangle \\ &\quad - 2\eta_{t,h} \sum_{k \in S_t} p_{k,t} \langle w_{t,h}^k - w^*, \nabla F_k(w_{t,h}^k) \rangle \end{aligned}$$

By Cauchy-Schwarz inequality and AM-GM inequality, we have

$$\begin{aligned} &-2\langle \bar{w}_{t,h} - w_{t,h}^k, \nabla F_k(w_{t,h}^k) \rangle \\ &\leq \frac{1}{\eta_{t,h}} \|\bar{w}_{t,h} - w_{t,h}^k\|^2 + \eta_{t,h} \|\nabla F_k(w_{t,h}^k)\|^2 \end{aligned}$$

By μ -convexity of F_k , we have,

$$\begin{aligned} &-\langle w_{t,h}^k - w^*, \nabla F_k(w_{t,h}^k) \rangle \\ &\leq -(F_k(w_{t,h}^k) - F_k(w^*)) - \frac{\mu}{2} \|\bar{w}_{t,h} - w^*\|^2 \end{aligned}$$

plug B_1, B_2 into A_1 :

$$\begin{aligned}
 A_1 &\leq (1 - \mu\eta_{t,h}) \|\bar{w}_{t,h} - w^*\|^2 + \sum_{k \in S_t} p_{k,t} \|\bar{w}_{t,h} - w_{t,h}^k\|^2 \\
 &\quad + \underbrace{4L\eta_{t,h}^2 \sum_{k \in S_t} p_{k,t} (F_k(w_{t,h}^k) - E[F_k(w_k^*)])}_{C_1} \\
 &\quad - \underbrace{2\eta_{t,h} \sum_{k \in S_t} p_{k,t} (F_k(w_{t,h}^k) - F_k(w^*))}_{C_2}
 \end{aligned}$$

where the last inequality results from L -smoothness of F_k . Next, we quantify the degree of non-iid:

$$\Gamma_{k,t} = E[F_k(w^*)] - E[F_k(w_k^*)] \quad (12)$$

where $k \in S_t$.

$$\begin{aligned}
 C_1 - C_2 &\leq 4L\eta_{t,h}^2 \sum_{k \in S_t} p_{k,t} \Gamma_{k,t} \\
 &\quad - 2\eta_{t,h}(1 - 2L\eta_{t,h}) \underbrace{\sum_{k \in S_t} p_{k,t} (F_k(w_{t,h}^k) - F_k(w^*))}_D
 \end{aligned}$$

We define $\gamma = 2\eta_{t,h}(1 - 2L\eta_{t,h})$. If $\eta_{t,h} \leq \frac{1}{4L}$, $\eta_{t,h} \leq \gamma \leq 2\eta_{t,h}$.

$$\begin{aligned}
 D &\geq - \sum_{k \in S_t} p_{k,t} [\eta_{t,h}L(F_k(\bar{w}_{t,h}) - E[F_k(w_k^*)]) \\
 &\quad + \frac{1}{2\eta_{t,h}} \|\bar{w}_{t,h} - w_{t,h}^k\|^2] \\
 &\quad + \sum_{k \in S_t} p_{k,t} (F_k(\bar{w}_{t,h}) - F_k(w^*))
 \end{aligned}$$

where the first inequality results from the convexity of $F_k(\cdot)$, the second and last inequality results from AM-GM inequality and L -smoothness. Next, we plug into $C_1 - C_2$

$$C_1 - C_2 \leq 6L\eta_{t,h}^2 \sum_{k \in S_t} p_{k,t} \Gamma_{k,t} + \sum_{k \in S_t} p_{k,t} \|\bar{w}_{t,h} - w_{t,h}^k\|^2$$

The inequality results from (1) $\sum_{k \in S_t} p_{k,t} (F_k(\bar{w}_{t,h}) - F_k(w^*)) \geq 0$ and $\eta_{t,h}L - 1 \leq -\frac{3}{4} < 0$;
(2) $\Gamma_{k,t} \geq 0$ and $4L\eta_{t,h}^2 + \gamma\eta_{t,h}L \leq 6\eta_{t,h}^2L$; (3) $\frac{\gamma}{2\eta_{t,h}} \leq 1$. Plug $C_1 - C_2$ into A_1 ,

$$\begin{aligned}
 A_1 &\leq (1 - \mu\eta_{t,h}) \|\bar{w}_{t,h} - w^*\|^2 + 6L\eta_{t,h}^2 \sum_{k \in S_t} p_{k,t} \Gamma_{k,t} \\
 &\quad + 2 \sum_{k \in S_t} p_{k,t} \|\bar{w}_{t,h} - w_{t,h}^k\|^2
 \end{aligned}$$

in which we have,

$$E \sum_{k \in S_t} p_{k,t} \|\bar{w}_{t,h} - w_{t,h}^k\|^2 \leq Q^2(H-1)^2 \eta_{t,h}^2 \sum_{k \in S_t} p_{k,t} \frac{G^2}{|\zeta_{t,h}^k|} \quad (13)$$

We take $\eta_{t,h'} \leq \eta_{t,0} = \eta_{t-1,H}$ with $0 \leq h' \leq H-1$ and $0 \leq h \leq H-1$. In the third inequality, we use the assumption $E \|f_k(w, x_{k,j})\|^2 \leq G^2$. In the last inequality, we assume that $\eta_{t,0} \leq Q\eta_{t,h'}$. Therefore, we bound A_1 as:

$$E[A_1] \leq (1 - \mu\eta_{t,h}) \|\bar{w}_{t,h} - w^*\|^2 + 6L\eta_{t,h}^2 \sum_{k \in S_t} p_{k,t} \Gamma_{k,t}$$

$$+ 2Q^2(H-1)^2\eta_{t,h}^2 \sum_{k \in S_t} p_{k,t} \frac{G^2}{|\zeta_{t,h}^k|} \quad (14)$$

Assume that the loss function f satisfies $E \|\nabla f_k(w_{t,h}^k, x_{k,j}) - \nabla F_k(w_{t,h}^k)\|^2 \leq \sigma^2, \forall t, h$. Inspired by [74], we bound A_2 as,

$$E[A_2] \leq \eta_{t,h}^2 \sum_{k \in S_t} p_{k,t} \frac{\sigma^2}{|\zeta_{t,h}^k|} \quad (15)$$

In the inequality, we use the Jensen inequality.

From Formulas 13, 14, and 15, we have,

$$\begin{aligned} & E \|\bar{w}_{t,h+1} - w^*\| \\ & \leq (1 - \mu\eta_{t,h})E \|\bar{w}_{t,h} - w^*\|^2 + 6L\eta_{t,h}^2 \sum_{k \in S_t} p_{k,t} \Gamma_{k,t} \\ & \quad + 2Q^2(H-1)^2\eta_{t,h}^2 \sum_{k \in S_t} p_{k,t} \frac{G^2}{|\zeta_{t,h}^k|} + \eta_{t,h}^2 \sum_{k \in S_t} p_{k,t} \frac{\sigma^2}{|\zeta_{t,h}^k|} \end{aligned}$$

We use the same batch size, i.e., $|\zeta_{t,h}^k| = b$, and then, we have:

$$\begin{aligned} & E \|\bar{w}_{t,h} - w^*\| \\ & = (1 - \mu\eta_{t,h})E \|\bar{w}_{t,h} - w^*\|^2 \\ & \quad + \eta_{t,h}^2 (6L \sum_{k \in S_t} p_{k,t} \Gamma_{k,t} + 2Q^2(H-1)^2 \frac{G^2}{b} + \frac{\sigma^2}{b}) \end{aligned}$$

In addition, we exploit Γ to represent $\max_{t \in \{1, \dots, T\}} \sum_{k \in S_t} p_{k,t} \Gamma_{k,t}$, and we have:

$$\begin{aligned} E \|\bar{w}_{t,h} - w^*\| & \leq (1 - \mu\eta_{t,h})E \|\bar{w}_{t,h} - w^*\|^2 \\ & \quad + \eta_{t,h}^2 (6L\Gamma + 2Q^2(H-1)^2 \frac{G^2}{b} + \frac{\sigma^2}{b}) \end{aligned}$$

Let $B = 6L\Gamma + 2Q^2(H-1)^2 \frac{G^2}{b} + \frac{\sigma^2}{b}$, which is a constant value, and we have:

$$E \|\bar{w}_{t,h} - w^*\| = (1 - \mu\eta_{t,h})E \|\bar{w}_{t,h} - w^*\|^2 + \eta_{t,h}^2 B$$

As $1 - \mu\eta_{t,h} \geq 0$, we have $\eta_{t,h} \leq \frac{1}{\mu}$. Within the inequality of D , we have $\eta_{t,h} \leq \frac{1}{4L}$. Thus,

$\eta_{t,h} \leq \min\{\frac{1}{\mu}, \frac{1}{4L}\}$ for any t . Let us assume that $\eta_{t,h} = \frac{\beta}{(t-1)H+h+\gamma}$, with $\beta > \frac{1}{\mu}$ and $\gamma > 0$. We

take $v \geq (\gamma+1) \|\bar{w}_{1,1} - w^*\|$, and we have $\|\bar{w}_{1,1} - w^*\| \leq \frac{v}{\gamma+1}$. Then, when $v = \frac{\beta^{m^2 B}}{\beta\mu-1}$, we have

$\|\bar{w}_{t,h} - w^*\| \leq \frac{v}{(t-1)H+h+\gamma}$ as:

$$\|\bar{w}_{t,h+1} - w^*\| \leq \frac{v}{(t-1)H+h+\gamma}$$

By L -smoothness of F , $E \|F(w_{t,h}) - F(w^*)\| \leq \frac{L}{2} E \|\bar{w}_{t,h} - w^*\|^2$, we have Theorem 1:

$$E \|F(w_{t,h}) - F(w^*)\| \leq \frac{L}{2} \frac{v}{(t-1)H+h+\gamma}$$

□

PROOF. Based on Theorem 5.6, when $v = \max\{(\gamma+1) \|\bar{w}_{1,1} - w^*\|, \frac{\beta^{m^2 B}}{\beta\mu-1}\}$, we have $E \|F(w_{T,H}) - F(w^*)\| \leq \frac{L}{2} \frac{v}{(t-1)H+h+\gamma}$. When $(\gamma+1) \|\bar{w}_{1,1} - w^*\| \leq \frac{\beta^{m^2 B}}{\beta\mu-1}$, $v = \frac{\beta^{m^2 B}}{\beta\mu-1}$. As B augments with $\sum_{k \in S_t} p_{k,t} \Gamma_{k,t}$, when $\sum_{k \in S_t} p_{k,t} \Gamma_{k,t}$ is smaller, the upper bound of $E \|F(w_{T,H}) - F(w^*)\|$ is smaller.

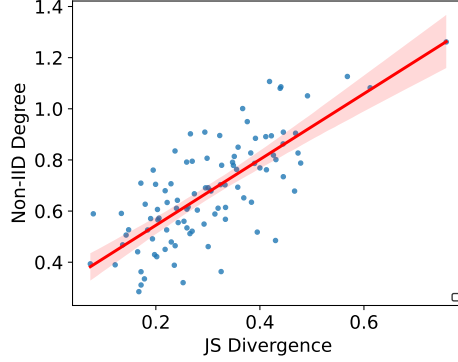


Fig. 7. Significant positive correlations have been found between JS divergence and non-IID degree

We denote $\Gamma_t^* = \sum_{k \in S_t} p_{k,t} \Gamma_{k,t}$ when $p_{k,t} = \frac{n_k}{\Gamma_{k,t}}$ and $\Gamma_t = \sum_{k \in S_t} p_{k,t} \Gamma_{k,t}$ when $p_{k,t} = \frac{n_k}{\sum_{k' \in S_t} n'_{k'}}$.

Then, we have:

$$\Gamma_t^* - \Gamma_t = \frac{\sum_{k \in S_t} n_k (\sum_{k' \in S_t} n'_{k'} - \Gamma_{k,t} \sum_{k' \in S_t} \frac{n'_{k'}}{\Gamma_{k',t}})}{(\sum_{k' \in S_t} \frac{n'_{k'}}{\Gamma_{k',t}}) (\sum_{k' \in S_t} n'_{k'})}$$

Let us denote $\delta = \sum_{k \in S_t} n_k (\sum_{k' \in S_t} n'_{k'} - \Gamma_{k,t} \sum_{k' \in S_t} \frac{n'_{k'}}{\Gamma_{k',t}})$, and we have:

$$\delta = \sum_{k \in S_t} \sum_{k' \in S_t} \frac{n_k n'_{k'} (\Gamma_{k',t} - \Gamma_{k,t})}{\Gamma_{k',t}}$$

When $k = k'$, we have $\Gamma_{k',t} - \Gamma_{k,t} = 0$. When $k \neq k'$, we have:

$$\frac{n_k n'_{k'} (\Gamma_{k',t} - \Gamma_{k,t})}{\Gamma_{k',t}} + \frac{n'_{k'} n_k (\Gamma_{k,t} - \Gamma_{k',t})}{\Gamma_{k,t}} = - \frac{n_k n'_{k'}}{\Gamma_{k',t} \Gamma_{k,t}} (\Gamma_{k,t} - \Gamma_{k',t})^2$$

Thus, we have $\delta \leq 0$ and $\Gamma_t^* - \Gamma_t \leq 0$ □

Correlation Analysis

In this study, we investigated the correlation between JS divergence and non-IID degree. We have evidenced the significance of the positive correlation between JS divergence and non-IID degree, supporting our hypothesis that higher JS divergence is associated with increased non-IID degree.

Based on Formula 12, we quantify the degree of non-IID as the difference between the global and expected local losses. We exploit a linear transformation of JS divergence in Formula 4. In order to analyze the correlation between two random variables, we calculate the Pearson correlation coefficient [75]. This statistical measure quantifies the linear relationship between the variables, providing a value between -1 and 1. A value closer to 1 indicates a strong positive correlation, while a value closer to -1 indicates a strong negative correlation. We also assessed the statistical significance of the correlation using p-values. The analysis yields a Pearson correlation coefficient of $R^{**} = 55.2\%$ ($N = 100, p\text{-value} = 9.27 \times 10^{-19} < 0.0001$), which implies strong linear relationship between JS divergence and the non-IID degree. This strong positive correlation is visualized in Figure 7.

Table 6. Performance comparison on CIFAR-10 and CIFAR-100 datasets with CNN model.

Method	Cifar10		Cifar100	
	Acc	Time	Acc	Time
FedDHAD (ours)	0.749	3074	0.423	4952
FedDH (ours)	0.744	3322	0.420	5018
FedAD (ours)	0.732	3632	0.412	5324
FedAS	0.705	3211	0.415	5172
FedKTL	0.684	6508	0.396	6593
AugFL	0.735	3490	0.407	5328

Comparitive Experiments

We evaluate the performance of our proposed methods against three recent advancements as objects for comparative experiments (e.g. FedAS [65], FedKTL [46], and AugFL [47]) using three key metrics: accuracy, training time. Accuracy measures the proportion of correctly classified samples in the test dataset using the trained global model. Training time is measured in seconds (s) and represents the time required to achieve a target accuracy level, which varies by dataset. We set target accuracies of 0.72 for CIFAR-10, and 0.41 for CIFAR-100. As shown in Table 7, FedDHAD consistently outperforms the three state-of-the-art, resulting in significantly higher accuracy (up to 1.93%) and training time (up to 2.12 times shorter).

In addition, we conduct an ablation study to compare the combination of FedDHAD and AEDFL [30]. We consider a decentralized FL system with 100 devices with an exponential graph topology. The results are shown in Table 7. The evaluation results demonstrate that the combination of AEDFL improves the accuracy by 1.9%. Furthermore, it can further improve the efficiency of FedDHAD (up to 64.0%). In the future, we will investigate in the combination of FedDHAD and other approaches to achieve superior performance.

Table 7. Ablation study results. “Acc” represents the convergence accuracy. “Time” refers to the training time (s) to achieve a target accuracy, i.e., 0.59 for LeNet with CIFAR10.

Method	Cifar10 & LeNet	
	Acc	Time
FedDHAD (ours)	0.633	2446
FedDH (ours)	0.621	2668
FedAD (ours)	0.595	3942
AEDFL+FedDHAD	0.645	880

Limitations

While FedDHAD can be exploited to efficiently train a model with distributed data, FedDHAD relies on central server for model aggregation. When the devices are connected using a decentralized topology without a central server, e.g., ring, it would be complicated to directly utilize FedDHAD for collaborative model training. In addition, FedDHAD is validated on traditional models, such as LeNet, CNN, further improvement is needed to adapt FedDHAD to other models, e.g., Transformers.

References

- [1] Peter Kairouz, H. Brendan McMahan, Brendan Avent, Aurélien Bellet, and Mehdi Bennis et al. Advances and open problems in federated learning. *Foundations and Trends® in Machine Learning*, 14(1-2):1–210, 2021.
- [2] Chunlu Chen, Ji Liu, Haowen Tan, Xingjian Li, Kevin I-Kai Wang, Peng Li, Kouichi Sakurai, and Dejing Dou. Trustworthy federated learning: Privacy, security, and beyond. pages 1–32, 2024.
- [3] Ji Liu, Chunlu Chen, Yu Li, Lin Sun, Yulun Song, Jingbo Zhou, Bo Jing, and Dejing Dou. Enhancing trust and privacy in distributed networks: a comprehensive survey on blockchain-based federated learning. *Knowledge and Information Systems*, pages 1–27, 2024.
- [4] Ji Liu, Jizhou Huang, Yang Zhou, Xuhong Li, Shilei Ji, Haoyi Xiong, and Dejing Dou. From distributed machine learning to federated learning: a survey. *Knowledge and Information Systems*, 64(4):885–917, 2022.
- [5] Official Journal of the European Union. General data protection regulation. <https://eur-lex.europa.eu/legal-content/EN/TXT/PDF/?uri=CELEX:32016R0679>, 2016. Online; accessed 09/05/2022.
- [6] Californians for Consumer Privacy. California consumer privacy act home page. <https://www.caprivacy.org/>, 2020. Online; accessed 09/05/2022.
- [7] Brendan McMahan, Eider Moore, Daniel Ramage, Seth Hampson, and Blaise Aguera y Arcas. Communication-efficient learning of deep networks from decentralized data. In *Artificial Intelligence and Statistics (AISTATS)*, pages 1273–1282, Fort Lauderdale, FL, USA, 2017. PMLR.
- [8] Ji Liu, Zhihua Wu, Danlei Feng, Minxu Zhang, Xinxuan Wu, Xuefeng Yao, Dianhai Yu, Yanjun Ma, Feng Zhao, and Dejing Dou. Heterps: Distributed deep learning with reinforcement learning based scheduling in heterogeneous environments. *Future Generation Computer Systems*, 148:106–117, 2023.
- [9] Mu Li, David G Andersen, Jun Woo Park, Alexander J Smola, Amr Ahmed, Vanja Josifovski, James Long, Eugene J Shekita, and Bor-Yiing Su. Scaling distributed machine learning with the parameter server. In *USENIX Symposium on Operating Systems Design and Implementation (OSDI)*, pages 583–598, 2014.
- [10] Jianyu Wang, Qinghua Liu, Hao Liang, Gauri Joshi, and H. Vincent Poor. Tackling the objective inconsistency problem in heterogeneous federated optimization. In *Advances in Neural Information Processing Systems (NeurIPS)*, volume 33, pages 7611–7623, Virtual Event, 2020. Curran Associates.
- [11] Ji Liu, Juncheng Jia, Beichen Ma, Chendi Zhou, Jingbo Zhou, Yang Zhou, Huaiyu Dai, and Dejing Dou. Multi-job intelligent scheduling with cross-device federated learning. *IEEE Transactions on Parallel and Distributed Systems*, 34(2):535–551, 2022.
- [12] Chendi Zhou, Ji Liu, Juncheng Jia, Jingbo Zhou, Yang Zhou, Huaiyu Dai, and Dejing Dou. Efficient device scheduling with multi-job federated learning. *AAAI Conf. on Artificial Intelligence*, 36(9):9971–9979, 2022.
- [13] Qinbin Li, Yiqun Diao, Quan Chen, and Bingsheng He. Federated learning on non-iid data silos: An experimental study. In *IEEE Int. Conf. on Data Engineering (ICDE)*, pages 965–978, Kuala Lumpur, Malaysia, 2022. IEEE.
- [14] Xiang Li, Kaixuan Huang, Wenhao Yang, Shusen Wang, and Zhihua Zhang. On the convergence of fedavg on non-iid data. In *Int. Conf. on Learning Representations (ICLR)*, pages 1–26, Addis Ababa, Ethiopia, 16 Sep 2024. OpenReview.net.
- [15] Tian Li, Anit Kumar Sahu, Manzil Zaheer, Maziar Sanjabi, Ameet Talwalkar, and Virginia Smith. Federated optimization in heterogeneous networks. In *Machine Learning and Systems (MLSys)*, volume 2, pages 429–450, Austin, TX, USA, 2020. mlsys.org.
- [16] Bent Fuglede and Flemming Topsøe. Jensen-shannon divergence and Hilbert space embedding. In *Int. Symposium on Information Theory (ISIT)*, page 31, Chicago, IL, United States, 2004. IEEE.
- [17] Solomon Kullback. *Information theory and statistics*. Courier Corporation, United States, 1997.
- [18] Ming Xie, Guodong Long, Tao Shen, Tianyi Zhou, Xianzhi Wang, Jing Jiang, and Chengqi Zhang. Multi-center federated learning. *arXiv preprint arXiv:2108.08647*, 26(1):481–500, 2021.
- [19] Keith Bonawitz, Hubert Eichner, Wolfgang Grieskamp, Dzmitry Huba, Alex Ingerman, Vladimir Ivanov, Chloé Kiddon, Jakub Konečný, Stefano Mazzocchi, Brendan McMahan, Timon Van Overveldt, David Petrou, Daniel Ramage, and Jason Roselander. Towards federated learning at scale: System design. In A. Talwalkar, V. Smith, and M. Zaharia, editors, *Proceedings of Machine Learning and Systems*, volume 1, pages 374–388, Stanford, California, United States, 2019. mlsys.org.
- [20] Nitish Srivastava, Geoffrey E. Hinton, Alex Krizhevsky, Ilya Sutskever, and Ruslan Salakhutdinov. Dropout: a simple way to prevent neural networks from overfitting. *Journal of Machine Learning Research*, 15(1):1929–1958, 2014.
- [21] Samuel Horvath, Stefanos Laskaridis, Mario Almeida, Ilias Leontiadis, Stylianos Venieris, and Nicholas Lane. Fjord: Fair and accurate federated learning under heterogeneous targets with ordered dropout. In *Advances in Neural Information Processing Systems (NeurIPS)*, volume 34, pages 12876–12889, Virtual Event, 2021. Curran Associates.
- [22] Nader Bouacida, Jiahui Hou, Hui Zang, and Xin Liu. Adaptive federated dropout: Improving communication efficiency and generalization for federated learning. In *IEEE Conf. on Computer Communications Workshops (INFOCOM WKSHPS)*, pages 1–6, Vancouver, BC, Canada, 2021. IEEE.

- [23] Dingzhu Wen, Ki-Jun Jeon, and Kaibin Huang. Federated dropout—a simple approach for enabling federated learning on resource constrained devices. *IEEE Wireless Communications Letters*, 11(5):923–927, 2022.
- [24] Durmus Alp Emre Acar, Yue Zhao, Ramon Matas, Matthew Mattina, Paul Whatmough, and Venkatesh Saligrama. Federated learning based on dynamic regularization. In *Int. Conf. on Learning Representations (ICLR)*, pages 1–36, Vienna, Austria, 2021. OpenReview.net.
- [25] Qinbin Li, Bingsheng He, and Dawn Song. Model-contrastive federated learning. In *IEEE/CVF Conf. on Computer Vision and Pattern Recognition (CVPR)*, pages 10713–10722, Virtual Event, 2021. IEEE.
- [26] Sai Praneeth Karimireddy, Satyen Kale, Mehryar Mohri, Sashank Reddi, Sebastian Stich, and Ananda Theertha Suresh. SCAFFOLD: Stochastic controlled averaging for federated learning. In *Int. Conf. on Machine Learning (ICML)*, volume 119, pages 5132–5143, Vienna, Austria, 2020. PMLR.
- [27] Benyuan Sun, Hongxing Huo, YI YANG, and Bo Bai. Partialfed: Cross-domain personalized federated learning via partial initialization. In *Advances in Neural Information Processing Systems (NeurIPS)*, volume 34, pages 23309–23320, Virtual Event, 2021. Curran Associates.
- [28] Jungwuk Park, Dong-Jun Han, Minseok Choi, and Jaekyun Moon. Sageflow: Robust federated learning against both stragglers and adversaries. In *Advances in Neural Information Processing Systems (NeurIPS)*, volume 34, pages 840–851, Virtual Event, 2021. Curran Associates.
- [29] Juncheng Jia, Ji Liu, Chendi Zhou, Hao Tian, Mianxiong Dong, and Dejing Dou. Efficient asynchronous federated learning with sparsification and quantization. *Concurrency and Computation: Practice and Experience*, 36(9):e8002, 2024.
- [30] Ji Liu, Tianshi Che, Yang Zhou, Ruoming Jin, Huaiyu Dai, Dejing Dou, and Patrick Valduriez. Aedfl: efficient asynchronous decentralized federated learning with heterogeneous devices. In *Proceedings of the 2024 SIAM International Conference on Data Mining (SDM)*, pages 833–841. SIAM, 2024.
- [31] Juncheng Jia, Ji Liu, Chao Huo, Yihui Shen, Yang Zhou, Huaiyu Dai, and Dejing Dou. Efficient federated learning with timely update dissemination. *Knowledge and Information Systems*, pages 1–38, 2025.
- [32] Ji Liu, Juncheng Jia, Tianshi Che, Chao Huo, Jiayang Ren, Yang Zhou, Huaiyu Dai, and Dejing Dou. Fedasmu: Efficient asynchronous federated learning with dynamic staleness-aware model update. In *Proceedings of the AAAI Conference on Artificial Intelligence*, volume 38, pages 13900–13908, 2024.
- [33] Qiang Yang, Yang Liu, Tianjian Chen, and Yongxin Tong. Federated machine learning: Concept and applications. *ACM Transactions on Intelligent Systems and Technology (TIST)*, 10(2):1–19, 2019.
- [34] Mingzhao Yang, Shangchao Su, Bin Li, and Xiangyang Xue. Exploring one-shot semi-supervised federated learning with pre-trained diffusion models. In *Proceedings of the AAAI Conference on Artificial Intelligence*, volume 38, pages 16325–16333, 2024.
- [35] Saber Salehkaleybar, Arsalan Sharifnassab, and S. Jamaloddin Golestani. One-shot federated learning: Theoretical limits and algorithms to achieve them. *Journal of Machine Learning Research*, 22(189):1–47, 2021.
- [36] Hubert Eichner, Tomer Koren, Brendan McMahan, Nathan Srebro, and Kunal Talwar. Semi-cyclic stochastic gradient descent. In *Int. Conf. on Machine Learning (ICML)*, pages 1764–1773, Long Beach, California, United States, 2019. PMLR.
- [37] Bruno Casella, Roberto Esposito, Carlo Cavazzoni, and Marco Aldinucci. Benchmarking fedavg and fedcurv for image classification tasks. *arXiv preprint arXiv:2303.17942*, 2023.
- [38] Yuhang Chen, Wenke Huang, and Mang Ye. Fair federated learning under domain skew with local consistency and domain diversity. In *Proceedings of the IEEE/CVF Conference on Computer Vision and Pattern Recognition*, pages 12077–12086, 2024.
- [39] Jiayin Jin, Jiayang Ren, Yang Zhou, Lingjuan Lv, Ji Liu, and Dejing Dou. Accelerated federated learning with decoupled adaptive optimization. In *Int. Conf. on Machine Learning (ICML)*, volume 162, pages 10298–10322, Baltimore, Maryland, United States, 2022. PMLR.
- [40] Mikhail Khodak, Maria-Florina F Balcan, and Ameet S Talwalkar. Adaptive gradient-based meta-learning methods. In *Advances in Neural Information Processing Systems (NeurIPS)*, volume 32, pages 1–12, Vancouver, BC, Canada, 2019. Curran Associates.
- [41] Virginia Smith, Chao-Kai Chiang, Maziar Sanjabi, and Ameet S Talwalkar. Federated multi-task learning. In *Advances in Neural Information Processing Systems (NeurIPS)*, volume 30, pages 1–11, Long Beach, CA, United States, 2017. Curran Associates.
- [42] Qinbin Li, Bingsheng He, and Dawn Song. Adversarial collaborative learning on non-iid features. In *International Conference on Machine Learning*, pages 19504–19526. PMLR, 2023.
- [43] Wenke Huang, Mang Ye, Zekun Shi, and Bo Du. Generalizable heterogeneous federated cross-correlation and instance similarity learning. *IEEE Transactions on Pattern Analysis and Machine Intelligence*, 46(2):712–728, 2023.
- [44] Mikhail Yurochkin, Mayank Agarwal, Soumya Ghosh, Kristjan Greenewald, Nghia Hoang, and Yasaman Khazaeni. Bayesian nonparametric federated learning of neural networks. In *Int. Conf. on Machine Learning (ICML)*, volume 97,

- pages 7252–7261, Long Beach, California, United States, 2019. PMLR.
- [45] Tao Lin, Lingjing Kong, Sebastian U Stich, and Martin Jaggi. Ensemble distillation for robust model fusion in federated learning. In *Advances in Neural Information Processing Systems (NeurIPS)*, volume 33, pages 2351–2363, Virtual Event, 2020. Curran Associates.
- [46] Jianqing Zhang, Yang Liu, Yang Hua, and Jian Cao. An upload-efficient scheme for transferring knowledge from a server-side pre-trained generator to clients in heterogeneous federated learning. In *Proceedings of the IEEE/CVF Conference on Computer Vision and Pattern Recognition*, pages 12109–12119, 2024.
- [47] Sheng Yue, Zerui Qin, Yongheng Deng, Ju Ren, Yaoxue Zhang, and Junshan Zhang. Augfl: Augmenting federated learning with pretrained models. *arXiv preprint arXiv:2503.02154*, 2025.
- [48] Yan Kang, Tao Fan, Hanlin Gu, Xiaojin Zhang, Lixin Fan, and Qiang Yang. Grounding foundation models through federated transfer learning: A general framework. *arXiv preprint arXiv:2311.17431*, 2023.
- [49] Pengwei Xing, Songtao Lu, Lingfei Wu, and Han Yu. Big-fed: Bilevel optimization enhanced graph-aided federated learning. In *Int. Workshop on Federated Learning for User Privacy and Data Confidentiality*, pages 1–8, Virtual Event, 2021. PMLR.
- [50] Yuang Jiang, Shiqiang Wang, Victor Valls, Bong Jun Ko, Wei-Han Lee, Kin K Leung, and Leandros Tassioulas. Model pruning enables efficient federated learning on edge devices. *IEEE Transactions on Neural Networks and Learning Systems (TNNLS)*, 1(1):1–22, 2022.
- [51] Sameer Bibikar, Haris Vikalo, Zhangyang Wang, and Xiaohan Chen. Federated dynamic sparse training: Computing less, communicating less, yet learning better. In *AAAI Conf. on Artificial Intelligence*, pages 6080–6088, Virtual Event, 2022. AAAI Press.
- [52] Yue Tan, Guodong Long, Jie Ma, Lu Liu, Tianyi Zhou, and Jing Jiang. Federated learning from pre-trained models: A contrastive learning approach. In *Advances in Neural Information Processing Systems (NeurIPS)*, pages 1–20, New Orleans, Louisiana, United States, 2022. Curran Associates.
- [53] Fan Lai, Xiangfeng Zhu, Harsha V Madhyastha, and Mosharaf Chowdhury. Oort: Efficient federated learning via guided participant selection. In *USENIX Symposium on Operating Systems Design and Implementation (OSDI)*, pages 19–35, 2021.
- [54] Moming Duan, Duo Liu, Xianzhang Chen, Yujuan Tan, Jinting Ren, Lei Qiao, and Liang Liang. Astraea: Self-balancing federated learning for improving classification accuracy of mobile deep learning applications. In *IEEE Int. Conf. on Computer Design (ICCD)*, pages 246–254, 2019.
- [55] Miao Yang, Hua Qian, Ximin Wang, Yong Zhou, and Hongbin Zhu. Client selection for federated learning with label noise. *IEEE Transactions on Vehicular Technology*, 71(2):2193–2197, 2021.
- [56] Hong Zhang, Ji Liu, Juncheng Jia, Yang Zhou, and Huaiyu Dai. FedDUAP: Federated learning with dynamic update and adaptive pruning using shared data on the server. In *Int. Joint Conf. on Artificial Intelligence (IJCAI)*, pages 1–7, 2022. To appear.
- [57] Ji Liu, Juncheng Jia, Hong Zhang, Yuhui Yun, Leye Wang, Yang Zhou, Huaiyu Dai, and Dejing Dou. Efficient federated learning using dynamic update and adaptive pruning with momentum on shared server data. *ACM Trans. on Intelligent Systems and Technology*, 2024.
- [58] Miao Yang, Ximin Wang, Hua Qian, Yongxin Zhu, Hongbin Zhu, Mohsen Guizani, and Victor Chang. An improved federated learning algorithm for privacy-preserving in cybertwin-driven 6G system. *IEEE Transactions on Industrial Informatics*, 18(10):6733–6742, 2022.
- [59] Martin Zinkevich, Markuss Weimer, Alexander J Smola, and Lihong Li. Parallelized stochastic gradient descent. In *Advances in Neural Information Processing Systems (NeurIPS)*, volume 23, pages 1–37, Vancouver, British Columbia, Canada, 2010. Curran Associates.
- [60] Saeed Ghadimi and Mengdi Wang. Approximation methods for bilevel programming. *arXiv preprint arXiv:1802.02246*, 2018.
- [61] Mingyi Hong, Hoi-To Wai, Zhaoran Wang, and Zhuoran Yang. A two-timescale framework for bilevel optimization: Complexity analysis and application to actor-critic. *arXiv preprint arXiv:2007.05170*, 2020.
- [62] Mingbao Lin, Rongrong Ji, Yan Wang, Yichen Zhang, Baochang Zhang, Yonghong Tian, and Ling Shao. Hrank: Filter pruning using high-rank feature map. In *IEEE/CVF Conf. on Computer Vision and Pattern Recognition (CVPR)*, pages 1529–1538, Seattle, WA, United States, 2020. IEEE.
- [63] Gang Yan, Hao Wang, and Jian Li. Seizing critical learning periods in federated learning. In *AAAI Conf. on Artificial Intelligence*, pages 1–8, Virtual Event, 2022. AAAI Press. To appear.
- [64] Zeru Zhang, Jiayin Jin, Zijie Zhang, Yang Zhou, Xin Zhao, Jiaxiang Ren, Ji Liu, Lingfei Wu, Ruoming Jin, and Dejing Dou. Validating the lottery ticket hypothesis with inertial manifold theory. *Advances in Neural Information Processing Systems (NeurIPS)*, 34:30196–30210, 2021.
- [65] Xiyuan Yang, Wenke Huang, and Mang Ye. Fedas: Bridging inconsistency in personalized federated learning. In *Proceedings of the IEEE/CVF Conference on Computer Vision and Pattern Recognition*, pages 11986–11995, 2024.

- [66] Alex Krizhevsky, Geoffrey Hinton, et al. Learning multiple layers of features from tiny images, 2009.
- [67] Yuval Netzer, Tao Wang, Adam Coates, Alessandro Bissacco, Bo Wu, and Andrew Y Ng. Reading digits in natural images with unsupervised feature learning. In *NIPS Workshop on Deep Learning and Unsupervised Feature Learning*, pages 1–9, Granada, Spain, 2011. Curran Associates.
- [68] Ya Le and Xuan Yang. Tiny imagenet visual recognition challenge. *CS 231N*, 7(7):3, 2015.
- [69] Yann LeCun, Bernhard Boser, John Denker, Donnie Henderson, Richard Howard, Wayne Hubbard, and Lawrence Jackel. Handwritten digit recognition with a back-propagation network. In *Advances in Neural Information Processing Systems (NeurIPS)*, volume 2, pages 1–9, Denver, CO, United States, 1989. American Institute of Physics.
- [70] Karen Simonyan and Andrew Zisserman. Very deep convolutional networks for large-scale image recognition. In *Int. Conf. on Learning Representations (ICLR)*, pages 1–14, San Diego, CA, United State, 2015. OpenReview.net.
- [71] Kaiming He, Xiangyu Zhang, Shaoqing Ren, and Jian Sun. Deep residual learning for image recognition. In *IEEE/CVF Conf. on Computer Vision and Pattern Recognition (CVPR)*, pages 770–778, Paradise, Nevada, United States, 2016. IEEE.
- [72] Ji Liu, Jiaxiang Ren, Ruoming Jin, Zijie Zhang, Yang Zhou, Patrick Valduriez, and Dejing Dou. Fisher information-based efficient curriculum federated learning with large language models. In *Empirical Methods in Natural Language Processing (EMNLP)*, pages 1–27, 2024.
- [73] Tianshi Che, Ji Liu, Yang Zhou, Jiaxiang Ren, Jiwen Zhou, Victor S Sheng, Huaiyu Dai, and Dejing Dou. Federated learning of large language models with parameter-efficient prompt tuning and adaptive optimization. In *Empirical Methods in Natural Language Processing (EMNLP)*, pages 1–18, 2023.
- [74] Ofer Dekel, Ran Gilad-Bachrach, Ohad Shamir, and Lin Xiao. Optimal distributed online prediction using mini-batches. *Journal of Machine Learning Research*, 13(1):165–202, 2012.
- [75] Jacob Benesty, Jingdong Chen, and Yiteng Huang. On the importance of the pearson correlation coefficient in noise reduction. *IEEE Transactions on Audio, Speech, and Language Processing*, 16(4):757–765, 2008.